TITLE

Harmony COVID-19: a ready-to-use kit, low-cost detector, and smartphone app for point-of-care SARS-CoV-2 RNA detection

ONE SENTENCE SUMMARY Harmony COVID-19: point-of-care SARS-CoV-2 RNA detection

AUTHORS

Nuttada Panpradist[1,2], Robert G. Atkinson[1], Michael Roller[1], Enos Kline[1], Qin Wang[1], Ian T. Hull[1], Jack H. Kotnik[1,3], Amy K. Oreskovic[1], Crissa Bennett[1], Daniel Leon[1], Victoria Lyon[3], Peter D. Han[4,5], Lea M. Starita[4,5], Matthew J. Thompson[3], Barry R. Lutz[1]*

AFFILIATIONS

1 Department of Bioengineering,

2 Global Health for Women, Adolescents, and Children, School of Public Health,

3 Department of Family Medicine,

4 Department of Genome Sciences, University of Washington, Seattle, WA, USA

5 Brotman Baty Institute for Precision Medicine, Seattle, WA, USA

*** CORRESPONDING AUTHOR**

B. R. L. (blutz@uw.edu)

3720 15th Ave NE, Campus Box 355061, Seattle, Washington, United States 98195

ABSTRACT (149 words)

RNA amplification tests allow sensitive detection of SARS-CoV-2 infection, but their complexity and cost are prohibitive for expanding COVID-19 testing. We developed "Harmony COVID-19", a point-of-care test using inexpensive consumables, ready-to-use reagents, and a simple device that processes up to 4 samples simultaneously. Our lyophilized reverse-transcription, loop-mediated isothermal amplification (RT-LAMP) can detect as little as 15 SARS-CoV-2 RNA copies per reaction, and it can report as early as 17 min for samples with high viral load (2×10^5 RNA copies per reaction). Analysis of RNA extracted from clinical nasal specimens (n = 101) showed 95% concordance with RT-PCR, including 100% specificity in specimens positive for other viruses and bacteria. Analysis of contrived samples in the nasal matrix showed detection of 92% or 100% in samples with ≥20 or ≥100 particles per reaction, respectively. Usability testing showed 95% accuracy by healthcare workers operating the test for the first time.

WORD COUNT (9,878 words)

INTRODUCTION

In 2019, an outbreak in China of SARS-CoV-2, the causative pathogen of COVID-19, rapidly became a global pandemic(*1*), and after a year it has infected 100 million people and killed 2 million people(*2*). Multiple measures have been used to contain the spread of COVID-19. Governments imposed universal "stay-home" orders to minimize transmission(*3*) which in turn has harmed mental health, social life, and the economy(*4*). It has been proposed(*5*) and demonstrated(*6*) that widespread COVID-19 testing and contact tracing could be a solution for re-openings, allowing subsets of a community to resume work and begin to restore the economy. Moreover, testing is essential for re-opening of international borders. Several countries have enforced a “fit-to-fly” policy; international travelers must test negative for COVID-19 within 72h before boarding international flights(*7*). Fast and sensitive point-of-care (**POC**) testing could facilitate the safe return to functioning domestic and international economies. POC testing could allow testing to expand to geographic regions that have limited access to centralized laboratory facilities, enable essential businesses to regularly test employees, and allow easy and efficient community testing by public health officials and clinics. Importantly, POC testing is critical in settings that require rapid turnaround time such as emergency urgent care facilities or points of introduction such as airports.

66 Here, we report the development of Harmony COVID-19 — a complete moderate-
67 throughput sample-to-result system for sensitive POC detection of SARS-CoV-2 RNA.
68 Harmony simplifies testing with ready-to-use assay reagents, an easy-to-use dedicated
69 smartphone interface, and an inexpensive isothermal heater/detector device to enable
70 POC testing. The assay includes three redundant SARS-CoV-2 targets to avoid false
71 negatives due to viral mutation and an internal amplification control (**IAC**) in each test to
72 avoid false negatives in case of assay failure. The heater/detector detects two-color
73 real-time fluorescence for the SARS-CoV-2 redundant targets and IAC, and results are
74 automatically reported on the smartphone. We evaluated the system using two panels
75 of specimens - a panel of extracted nasal specimens from individuals with respiratory
76 symptoms, and a blinded panel of contrived specimens from the XPRIZE Rapid Covid
77 Testing competition – and we conducted usability testing of Harmony by healthcare
78 workers (**HCWs**). These evaluations have demonstrated that Harmony is a complete
79 system for sample-to-result testing that is high performance and sufficiently simple for
80 CLIA-waived settings.
81

82 **RESULTS**

83 **Workflow and operation of COVID-19 Harmony**

84 The Harmony test kit and detector were engineered for low cost and simplicity of use to
85 enable POC testing (**Fig.1a**). The test involves taking a nasal swab, eluting the swab in
86 a lysis buffer, and transferring the buffer to a reaction tube containing ready-to-use

87 reagents. The reagent tube is inserted into the custom-designed heater/reader operated
88 by a cell phone that provides instructions and displays the result.
89
90 The Harmony assay uses a unique variation of reverse transcription loop-mediated
91 isothermal amplification (**RT-LAMP**) that allows fluorescence detection of multiple
92 targets in the same reaction. The assay amplifies three genomic regions of the SARS-
93 CoV-2 nucleocapsid phosphoprotein reported by a green fluorescence signal (FAM) and
94 an engineered internal amplification control (**IAC**) reported by a red fluorescence signal
95 (TEX 615, alternative for Texas Red®). For samples with no target (**Fig. 1B**, left; NTC),
96 detection of the IAC confirms that the reaction was functional; absence of target and
97 IAC indicates a failed reaction. For samples with SARS-CoV-2 RNA (**Fig. 1B**, middle;
98 200 copies/rxn), the green signal indicates a positive test, regardless of whether IAC is
99 detected. Harmony using dry reagents detects down to 200 copies of SARS-CoV-2
100 RNA on a swab (**Fig. 1B**, right; ~20 copies/rxn, corresponding to 0.5 copies/μL). Real-
101 time detection reports a positive sample as soon as the target signal appears, allowing
102 detection in <30 min for samples ≥2000 copies per swab (**Fig. 1C**), with earlier results
103 for higher viral load. The three SARS-CoV-2 targets are reported into the green
104 fluorescence channel to provide a triply-redundant assay to make it robust against viral
105 mutations (**Fig. 1D**). A positive test result is reported when any of the three SARS-CoV-
106 2 targets are present, and a negative test result is reported if SARS-CoV-2 RNA is
107 undetected, and the IAC is detected. If neither target nor IAC is detected, it indicates a

108 test failure, and the result is reported as indeterminate (**IND**). **table S1** lists the
109 sequences of primers/probes used in this RT-LAMP assay.
110
111 **Development and analytical sensitivity of ready-to-use reagents.**
112 We have developed a lyophilized RT-LAMP mixture that contains primers, sequence-
113 specific fluorescence probes, IAC DNA template, polymerases, supporting proteins, and
114 co-factors (**Fig. 2A**) and is activated by adding the nasal swab eluate containing
115 additional buffer, salts, and detergent. We initially screened excipient formulations that
116 can preserve enzymatic activity and do not significantly interfere with the primer or
117 probe behaviors. Mannitol did not drastically impact the core assay compared to
118 trehalose at the same concentration (**fig. S1**) and did not require increasing the reaction
119 temperature to maintain the assay speed. Using a commercial real-time thermal cycler,
120 lyophilized RT-LAMP detected down to 15 RNA copies/rxn (0.38 copies/μL), and IAC
121 was detected in all negative samples (**Fig. 2B**). RT-LAMP amplification of $2x10^5$ RNA
122 copies/rxn using the dry reagents generated detectable signal in 17 min (**Fig. 2C**). We
123 subsequently tested our in-house lyophilized reagents on a larger number of technical
124 replicates of SARS-CoV-2 RNA at 20 copies/rxn using multiple batches, and 90%
125 (36/40, 95% confidence interval (**CI**): 76-97%) were amplified (**Fig. 2D**). Medians of time
126 to detection for FAM and TEX 615 signals were 28.6 min (range: 28.0-29.4) and 31.7
127 min (range: 31.1-32.7), respectively. In the presence of simulated nasal matrix (salt,
128 mucin, human DNA), we observed a 10-min delay in amplification of both SARS-CoV-2
129 RNA and IAC DNA (**Fig. 2E**), but all targets were detected correctly. Greater

130 interference or other harm to the reaction will further delay IAC amplification; thus, the
131 IAC serves as an indicator of the reaction's function and can prevent reporting false
132 negatives due to interference or damaged reagents. By setting a 1-hour reaction time,
133 the assay can suffer some delay while still correctly identifying positive samples.
134 Specificity testing against closely-related pathogens MERS and SARS-CoV-1 showed
135 no cross-reactivity (**fig. S2**).
136
137 **Hardware: housing and real-time fluorescence reader device**
138 The Harmony system includes a heater/detector device controlled by a dedicated cell
139 phone and plastic housing with a sample setup station (**Fig. 3A**). The heater/detector
140 device (**Fig. 3B**) includes an aluminum heater block with four wells and a spring-loaded
141 heated lid to prevent condensation. A proportional integral derivative (**PID**) feedback
142 loop running on a microcontroller allows recovery of the temperature setpoint within 3-4
143 min after disturbance from opening the lid (**Fig. 3C**). Two LEDs (**Fig. 3D**) provide the
144 excitation light by shining down through the top of each sample tube. Fluorescence
145 emission passes through holes drilled on the side of the heater block. Each sample well
146 has an emission filter/photodiode set on each side to detect two emission wavelengths
147 (**Fig. 3E**). A blue LED (dominant wavelength 470nm) is used to excite FAM, and the
148 emission photodiode sits behind a dielectric 550nm longpass filter. A yellow LED
149 (dominant wavelength 587nm) is used to excite TEX 615, and a second emission
150 photodiode sits behind a 630nm longpass dielectric filter.
151

152 **Thermostable Inorganic Pyrophosphatase enables real-time LAMP detection in**
153 **the Harmony COVID-19 device**
154 RT-LAMP generates inorganic pyrophosphates that precipitate from the solution. The
155 cloudiness created by precipitates has been used as a visual readout signal for
156 LAMP(*8*), but here the cloudiness scattered light and caused non-specific signals in
157 NTC samples (**Fig. 3F,** top) when tested on device. Adding inorganic pyrophosphatase
158 in the RT-LAMP reaction eliminated built-up pyrophosphate and prevented non-specific
159 signal in negative reactions (**Fig. 3F,** bottom). Interestingly, this effect was not observed
160 when the reaction was tested in the commercial thermal cycler (BioRad CFX96).
161
162 **Multi-purpose Android mobile app: instruction, temperature control, and real-time**
163 **analysis of results**
164 The phone software provides interactive guidance for setting up the test. It prompts the
165 user to input a sample ID by scanning a barcode, capturing a photo, or typing a sample
166 ID (**Fig. 4, A-D**). The software also carries out the closed-loop temperature control for
167 the heater block and lid heater, and it displays the status of the heater block to prompt
168 the user to insert the reaction tubes only after the heater reaches the reaction
169 temperature (**Fig. 4E)**. During the test run, the screen displays the test status ("analysis
170 in progress") and elapsed time, or it reports any detected errors ("failed run") (**Fig. 4F**).
171 Importantly, the software performs real-time data analysis that detects fluorescence
172 intensity rise above a dynamically and automatically computed background level.
173 Signals from SARS-CoV-2 can appear early in the test, especially for high viral loads,

174 and the real-time analysis allows reporting of positive tests immediately after they are
175 detected (**Fig. 4G**). Negative results and IND results are reported at the end of the test
176 run time (**Fig. 4H**). Software analysis is described in the Methods section.
177

178 **Evaluation using extracted RNA from clinical specimens**

179 Clinical specimens collected from individuals positive for SARS-CoV-2 (*n = 33*) or for
180 other pathogenic respiratory infections (*n = 68*) were re-tested by RT-qPCR(*9*) to
181 measure the SARS-CoV-2 viral load and provide the reference test result. Using RT-
182 qPCR, 68 specimens were confirmed to be SARS-CoV-2 negative (**Fig. 5A,** left), 30
183 specimens were confirmed to be SARS-CoV-2 positive (**Fig. 5A,** right), and three
184 previously-positive specimens were only detected by one RT-qPCR assay (either N1 or
185 N2) and classified as inconclusive (**INC, Fig. 5A,** middle). Specimens were tested in
186 duplicate on Harmony using the ready-to-use reagents (**Fig. 5A)**, arranged from low to
187 high virus concentration as determined by RT-qPCR. Out of 30 RT-qPCR-positive
188 specimens, Harmony detected 25 specimens in both technical replicates and 4
189 specimens in one of the two replicates. In the three RT-qPCR INC results, one sample
190 was detected by Harmony in one of the two replicates. Excluding the RT-qPCR INC
191 specimens and applying a stringent requirement for both Harmony replicates to be
192 detected to report a positive test, Harmony achieved 95% accuracy (93/98, 95%CI: 88-
193 98%), 83% sensitivity (25/30, 95%CI: 65-94%), and 100% specificity (68/68, 95%CI: 94-
194 100%). If replicates are treated independently, Harmony detected 54/60 positive
195 specimens (90% sensitivity, 95%CI: 79-96%). For specimens with ≥10 copies/rxn,

196 Harmony detected 24/25 specimens (96% sensitivity, 95%CI: 80-100%), and for
197 specimens with ≥40 copies/rxn, Harmony detected 18/18 specimens (100% sensitivity,
198 95%CI: 81-100%).
199 The clinical panel (**Fig. 5A**) included 68 specimens that were SARS-CoV-2 negative but
200 contained other respiratory pathogens including influenza, rhinovirus, and seasonal
201 coronavirus (**Fig. 5B**). Harmony correctly identified 68/68 specimens (**Fig. 5A,** left) as
202 negative (100%, 95%CI: 94-100% specificity). **Fig. 5C** summarizes the performance of
203 the extracted clinical specimens.
204
205 **Evaluation of contrived SARS-CoV-2 viral particle specimens without extraction** A
206 panel of 69 contrived samples from the COVID-19 XPRIZE competition were tested on
207 the Harmony system with ready-to-use reagents (**Fig. 5**, **D** and **E**). For SARS-CoV-2
208 virus in PBS, Harmony detected 100% of samples containing ≥50 SARS-CoV-2 viral
209 particles/rxn, and 89% of samples containing ≥20 viral particles/rxn in PBS (despite
210 PBS being a non-ideal buffer). In nasal matrix, Harmony COVID-19 detected 100% of
211 samples containing ≥100 viral particles/rxn, and 92% of samples containing ≥20 viral
212 particles/rxn. In human saliva, Harmony detected 100% of samples with ≥250 viral
213 particles/rxn and 58% with ≥20 viral particles/rxn. Harmony had zero false positives
214 across all samples.
215
216 **Feasibility testing: sample-to-result system tested by healthcare workers and**
217 **laboratory personnel**

218 To complete the system, we developed a test kit that included all components needed
219 for running a test, including the swab, elution buffer, a fluid transfer device, and a ready-
220 to-use reagent tube. Swabs were pre-loaded with SARS-CoV-2 DNA to serve as a
221 control sample to evaluate performance by HCWs and laboratory personnel (**LPs**).
222
223 In the first phase of user testing (**Fig. 6A**), we compared the accuracy and
224 reproducibility of two methods for transferring the eluate to the reaction tube when
225 operated by LPs *(n = 5*) and HCWs (such as nurses, medical students, and dental
226 students; *n = 10*). The first method (**Fig. 6B** and shown-previously in **Fig. 1**) used a
227 unified sampler-dispenser. The second method (**Fig. 6C**) used a transfer pipette to
228 transfer a fixed volume of fluid to the reaction tube. Regardless of the baseline skill of
229 operators, transfer pipettes yielded more reproducible recovered volumes than the
230 unified dispenser (F-test, $p < 0.001$). Recovered volumes of the two methods were not
231 significantly different between HCWs and LPs (student's t-test, two-sided, $p = 0.90$; **Fig.**
232 **6D**). User feedback on the transfer methods and preferences on tube sizes are
233 summarized in **table S2**.
234
235 Next, HCWs and LPs executed the full Harmony workflow on contrived SARS-CoV-2
236 DNA swab samples (**Fig. 6**). Using the transfer pipette workflow (**Fig. 6E**), the test
237 accuracy was 100% (10/10) for LPs and 95% (19/20) for HCWs. Surprisingly, we found
238 that the HCWs performed better than the LPs when using the unified dispenser system
239 (**Fig. 6F**), both accuracy and IND rates. HCWs had significantly lower (Z-test, two-tailed,

240 p<0.05) IND results (1/20) than LPs (3/10) when using the unified dispenser system.
241 Excluding IND results, the HCWs had 89% accuracy, higher than LPs with 71%
242 accuracy (Z-test, two-tailed, p <0.05), when using the unified dispenser system.

243 **DISCUSSION**

244 This work presents a combination of multi-disciplinary engineering (molecular,
245 mechanical, electrical, software, human interface design) to develop a complete system
246 for SARS-CoV-2 detection at the POC. The system is inexpensive and simple yet has
247 features comparable to laboratory-based tests (**Table 1A**). The assay has high
248 sensitivity and specificity in clinical and contrived specimens, and HCWs successfully
249 performed the workflow with high accuracy.

250 Harmony uses ready-to-use reagents that improve speed and accuracy for assay setup.
251 Unlike other lyophilized RT-LAMP[25], our lyophilized reagents are magnesium-free,
252 which prohibits any enzymatic activity that may occur before assay initiation. Our
253 lyophilized RT-LAMP is activated upon the addition of sample which contains
254 magnesium and detergent. Thus, it should be less prone to moisture degradation than
255 magnesium-containing lyophilized RT-LAMP.

256 The lyophilized Harmony assay detected as low as 15 copies/rxn of synthetic SARS-CoV-
257 2 RNA and detected all extracted RNA samples from clinical specimens at ≥40 copies/rxn.
258 Here, we used only 10μL RNA in 40μL reaction to allow head-to-head sensitivity
259 comparison to the CDC RT-PCR protocol that uses 5μL RNA in a 20μL reaction. The

260 lyophilized reagents can accommodate up to 40μL of sample (4x than used here), which
261 could further increase Harmony sensitivity.

262 Harmony lyophilized RT-LAMP is robust against simulated nasal matrix containing
263 mucin, salt, and human genomic DNA. The impact of salts and mucin was observed as
264 a delayed reaction time for both target and IAC. To account for this delay, we adjusted
265 the assay time to 90 min when analyzing specimens with nasal matrix. We found
266 excellent sensitivity when testing samples with ≥50 viral particles in nasal matrix
267 (estimated 1250 copies/swab for 1mL elution buffer and 40μL reaction), which would be
268 sufficient to detect SARS-CoV-2 in most nasal specimens (10^3-10^9 SARS-CoV-2
269 copies/swab) from individuals within the first 3-5 days after the symptom
270 onset[26]. Further, Harmony detected all samples with ≥100 viral particles in nasal matrix
271 (estimated 2500 copies/swab for 1mL elution buffer and 40μL reaction). While saliva
272 was not our intended specimen type, we found a moderate sensitivity when testing the
273 XPRIZE blinded saliva panel. Heat treatment of saliva shown to enable detection by RT-
274 PCR[27] would likely improve the sensitivity of our RT-LAMP in detecting SARS-CoV-2 in
275 saliva.

276 Isothermal amplification, like RT-LAMP in Harmony, is often promoted as ideal for POC
277 testing because it can be carried out using a constant temperature heat source, such as
278 a water bath, heat block, or even more novel sources (chemical heat source, sunlight,
279 body temperature)(*10*). However, reported tests often have other limitations that may
280 prevent their use in POC testing (**Table 1B**). Common limitations include use of
281 reagents use of refrigerated or frozen reagent stocks that must be formulated using

282 laboratory pipettes, manual steps for sample processing that require laboratory skill, or
283 detection steps that rely heavily on user interpretation or analysis by a user's cell phone.
284 Harmony is a complete sample-to-result system that uses ready-to-use reagents for
285 simple 1-minute setup and a dedicated device that reports results without extra post-
286 amplification steps or reliance on user interpretation.

287 Some RT-LAMP tests use end-point lateral flow strips for detection[28], which adds a user
288 step, but more importantly, should not be done at the POC because it exposes the
289 testing site to amplicons that will give false positive results in subsequent tests. Others
290 use in-tube detection by eye(*11*),(*11*) or using a cell phone(*12*) which increases the user
291 burden and could introduce additional sources of error. Real-time detection used in
292 Harmony COVID-19 removes the need for extra detection steps or user interpretation.
293 Real-time detection also allows Harmony to report positive results as soon as the
294 SARS-CoV-2 signal appears rather than waiting for an end-point detection method.
295 High viral load samples could be detected in as little as 20 min, which could enable
296 more timely infection control measures to limit viral spread. Harmony real-time detection
297 allows testing without opening tubes after amplification, requires no extra steps or
298 interpretation by the user, and allows reporting a positive sample earlier than end-point
299 detection methods.

300 The Harmony device automates heating, multiplexed detection, and data interpretation.
301 We integrated a simple heater with low-cost LEDs and sensors to enable real-time two-
302 color detection of RT-LAMP fluorescence in four independent sample wells. The device
303 costs <US$300 in parts for prototypes, while the lowest cost commercial RT-PCR

304 machine on the market is >US$5000(*13*). Moreover, the Harmony device is portable
305 and energy-efficient, requiring <15 watts and operable by USB power sources. These
306 features are attractive for use at the POC in the U.S. and resource-limited settings.

307 Lastly, the simple workflow and analysis of Harmony is appropriate for POC testing.
308 Test operation involves a few simple steps that take ~1 minute, and there are no further
309 user steps after starting the test. Here, HCWs were able to operate the tests without
310 training using only simple written instructions and watching the procedure on video. The
311 simplicity of the Harmony procedure and completeness of the stand-alone system can
312 be a significant advantage for onboarding to ambulatory care settings and potentially
313 community testing locations.

314 In this study, we evaluated the system using RNA extracted from clinical samples stored
315 in viral transport medium (**VTM**) and contrived specimens in unknown nasal and saliva
316 matrix (XPRIZE), which may not reflect performance in fresh clinical samples. These
317 samples were used due to the difficulty of obtaining fresh dry swabs intended for this
318 POC test, and RNA was extracted from clinical samples because VTM is irrelevant for
319 immediate testing at the POC. Nevertheless, this testing shows excellent analytical
320 reactivity to clinical specimens, lack of cross-reactivity with other respiratory pathogens,
321 analytical sensitivity comparable to the CDC RT-PCR, and resilience in the presence of
322 nasal matrix.

323 While our assay is relatively fast and sensitive, there is potential to improve
324 performance. We ran RT-LAMP at 64°C, which is 9°C above the optimal temperature
325 for the RT enzyme. We hypothesize that cooling of the heat block when the lid is open,

326 followed by a few minutes to ramp back up to 64°C, provided an opportunity for the RT
327 enzyme to operate. In contrast, the reaction speed of the temperature-stable DNA
328 polymerase in this assay is optimal at higher temperature. Thus, operating the device
329 with an initial 55°C step for optimal RT activity followed by a higher temperature step for
330 fast DNA amplification could increase sensitivity and/or speed.

331 The current design of RT-LAMP assay can be improved to include an IAC that is more
332 representative of the SARS-CoV-2 virus. We currently use a DNA IAC, which has been
333 used in several EUA assays[34], but the DNA control does not capture the potential failure
334 of the lysis and cDNA conversion processes. We are developing a new IAC that uses
335 RNA that can be packaged in a viral envelope. This modification may require re-
336 development of excipients that preserve the RT-LAMP enzymes and the enveloped
337 RNA.

338 POC tests like Harmony could provide rapid testing to enable the re-opening of
339 businesses, schools, and borders; but the need for POC testing extends beyond the
340 current emergency. As natural immunity and vaccination take hold, COVID-19 is likely
341 to become endemic with seasonal outbreaks. Tests such as Harmony will be necessary
342 not only to help identify individuals with SARS-CoV-2, but other respiratory pathogens
343 such as influenza and RSV, as the symptoms of these are similar. Prior to the current
344 SARS-CoV-2 pandemic, the yearly influenza infections caused nearly 30 million cases
345 in the U.S. alone, with 400,000 hospital admission and 35,000 deaths(*14, 15*). Indeed,
346 particularly when more typical patterns of respiratory infections occur, there will be a
347 need for tests that can perform multiplex testing for individuals presenting respiratory

348 symptoms. Tests such as Harmony will become a common practice for confirming
349 presence of viral infections that can be treated with antiviral therapies or that demand
350 infection control, as well as helping to reduce inappropriate use of antibiotics. Further,
351 test platforms developed for this pandemic could be more readily adapted to detect new
352 diseases to increase readiness for future pandemics. The advances in awareness and
353 acceptance of testing for infections at scale, and the technology platforms developed
354 will have ongoing benefit for COVID-19 control, reducing harm from other endemic
355 diseases, and fighting future pandemics.

356 **MATERIALS AND METHODS**

357 **Preparation of synthetic RNA standards**

358 MERS and SARS-CoV-1 plasmid standards (10006623 and 10006624, Integrated DNA
359 Technologies, Coralville, IA) were amplified using M13 PCR primers to generate DNA
360 templates tagged with T7 promoter sequences. DNA templates containing T7 promoter
361 sequences were transcribed using Hi-T7 RNA polymerase (M0658, New
362 England Biolabs, Lawley, MA) following the manufacturer's protocol, with 1 U/μL RNase
363 inhibitor (N2611, Promega, Madison, WI). Following transcription, 0.01U/μL DNase I
364 (EN0521, ThermoFisher Scientific, Waltham, MA) was added to each reaction, and
365 incubated at 37°C for 15 min. RNA transcripts were purified with Monarch RNA Cleanup
366 Kits (T2040, New England Biolabs). RNA was quantified on a Qubit 4 fluorometer
367 (Q32852, RNA HS Assay Kit, ThermoFisher Scientific, Waltham, MA), and checked for
368 length and integrity by electrophoresis on TapeStation (5067 RNA screening tape,
369 Agilent Technologies, Santa Clara, CA). RNA at 10^{10} copies/μL was stored in nuclease-

370 free water in single-use aliquots. SARS-CoV-2 RNA was prepared and quantified as
371 previously described(*16*).
372
373 **In-house polymerase production**
374 **Plasmid preparation:** The chimeric polymerase (TFv1) was generated by assembly
375 PCR using genomic material from *Thermus thermophilus* HB27 (ATCC BAA-163D-5™,
376 Gaithersburg, MD) and a synthetic gene fragment derived from *Thermodesulfatator*
377 *indicus* (*T. in*), (Integrated DNA Technologies, Coralville, IA), similar to the method
378 previously described(*17*). Briefly, a 3' terminal fragment of the *T.th* HB27 ***Pol*A** gene
379 downstream of the finger domain was amplified by PCR using Phusion® Hot Start Flex
380 DNA Polymerase (M0535L, New England Biolabs) with a modified forward primer
381 containing sequence overlap with the *T. in polA* gene fragment *(AA734-795,* codon
382 optimized for *E. coli)*. A chimeric sequence was then generated by assembly PCR. A
383 second*T.th* polymerase fragment, upstream of the finger domain and lacking the 3´to 5´
384 exonuclease domain, was similarly amplified and appended to the 5' end of the chimeric
385 fragment. The resultant sequence corresponds to a *T. th* DNA polymerase I fragment,
386 orthologous to the Stoffel fragment of *T.aq.* polymerase, with a replacement in the finger
387 domain derived from *T. in*. This gene was then cloned into the expression vector pET
388 His6 TEV LIC cloning vector (2B-T) (a gift from Scott Gradia, Plasmid # 29666,
389 Addgene, Watertown, MA) by ligation independent cloning(*18*). The annealed vector
390 and insert were transformed into T7 Express lysY/Iq Competent *E.* coli (C2987H, New

391 England Biolabs) per the manufacturer's protocol and plated on LB 100μg/mL
392 carbenicillin plates. Colony plasmid inserts were verified by Sanger sequencing.
393 **Protein expression and purification:** 50mL starter culture in LB broth with 100μg/mL
394 carbenicillin was inoculated with a sequence-verified colony and incubated at 30°C
395 overnight in a shaking incubator at 200rpm. The culture was centrifuged at 5,000 RCF
396 for 15 min and resuspended in an equivalent volume fresh LB carbenicillin media.
397 Flasks of 500mL LB broth with 100μg/mL carbenicillin were inoculated with 5mL of
398 resuspended starter culture and incubated at 37°C in a shaking incubator at 200rpm
399 until OD_{600} of 0.4-0.6 had been achieved. Cultures were induced with 0.4mg/mL of IPTG
400 and incubated for two hours then harvested by centrifugation at 5,000 RCF for 15 min,
401 decanted, and stored as cell pellets at –80°C until needed. Prior to purification, cell
402 pellets were resuspended in lysis buffer (20mM sodium phosphate pH7.4, 80mM NaCl,
403 1%*(v/v)* Triton (648466 Sigma, St. Louis, MO), and 1mg/mL lysozyme from chicken egg
404 white (Millipore Sigma, Burlington, MA)). Suspensions were heated at 37°C for 20 min,
405 then lysed by ultrasonic disruption using a Fisherbrand™ Model 120 Sonic
406 Dismembrator (Fisher Scientific, Waltham, MA) with two cycles of two second pulses at
407 50% amplitude for 2 min, while on ice. Lysates were heat-clarified at 65°C for 20 min,
408 followed by centrifugation at 20,000 RCF. The supernatant was collected and diluted
409 1:6 with sample diluent buffer (20mM sodium phosphate, 1.8M NaCl, pH 7.4) and
410 filtered with a 0.22 μm syringe filter (25-342 Olympus, Genesee Scientific, San Diego,
411 CA). The Purified clarified lysate was applied to a 1mL Hitrap Talon Crude column
412 (Cytiva, Marlborough, MA) and enriched per manufacturers default recommended

413 specifications using an ÄKTA start system with the Frac30 fraction collector (Cytiva).
414 Elution fractions were evaluated by A_{280} on a spectrophotometer (2200 Nanodrop,
415 Fisher Scientific) using the proteins expected molecular weight (63.062kDa) and
416 extinction coefficient (60,850m^2/mol) of the His-tagged polymerase. Elution fractions
417 containing protein were diluted 1:10 with 10mM sodium phosphate and applied to a 1mL
418 HiTrap® Heparin HP column and purified per the manufacturers recommended
419 specifications except for a modified binding buffer (10mM sodium phosphate, and
420 30mM NaCl, at pH 7). Fractions containing protein were concentrated and buffer
421 exchanged into storage buffer (17mM Tris-HCl, 167mM KCl, 17% glycerol pH7.5) using
422 an Amicon® Ultra-2 30K device (Millipore Sigma), as recommended by the
423 manufacturer. The recovered polymerase solution was then adjusted to 10mM Tris-HCl,
424 100mM KCl, 2mM DTT, 0.1%Triton X-100, 50%glycerol pH7.5. Polymerase purity was
425 evaluated by SDS-PAGE and spectrophotometry throughout purification.

426

427 **RT-LAMP assay design**

428 Alignment of SARS-CoV-2 sequences (available on NCBI up to January 2020) were
429 performed using Geneious (Auckland, New Zealand). Three sets of LAMP primers
430 (Harmony NC1, Harmony NC2, and Harmony NC3) were developed targeting the
431 22,285 – 28,517 (232 bases), 28,528 – 28,471 (213 bases), and 29,135 – 29,416 (281
432 bases) regions of the SARS-CoV-2 nucleocapsid phosphoprotein gene. *In-slico* analysis
433 showed that this primer design matched 100% of SARS-CoV-2 sequences and did not
434 have cross-reactivity to MERS and SARS-CoV-1. We used two detection probes, each

435 comprised of a fluorescent probe and its complementary quencher probe. For detection
436 of SARS-CoV-2 RNA amplification, we used FAM labeled detection probe and Iowa
437 Black™ quencher probe. For detection of IAC amplification, we used TEX 615 labeled
438 detection probe and BHQ2 labeled quencher probe. The primer and probe sequences
439 are listed in **table S1**.
440

441 **Lyophilization of RT-LAMP reagents**

442 Reactions containing 2x primers (3.2mM each FIP/BIP primer, 0.4mM each loop primer,
443 and 0.8mM each F3/B3 primer) and probes (0.4mM fluorophore probes and 0.6mM
444 quencher probes) in the presence of 5% *(v/v)* mannitol (OPS Diagnostics EXMN 500-
445 01), 10mM DTT, 1.4*μ*g DNA polymerase, 1.2U/*μ*L WarmStart RTx (M0380L, New
446 England Biolabs), 2.8mM each dNTP in 10mM Tris-HCl, pH 7.4, 2U/*μ*L RNase inhibitor
447 (N2615, Promega), 50mU/*μ*L thermostable inorganic pyrophosphatase (M0296L, New
448 England Biolabs), and 2500 copies/*μ*L IAC DNA were prepared in 20*μ*L aliquots of
449 0.2mL reagent tubes and lyophilized. Packages were stored in desiccant packets at -
450 20°C until use.
451

452 **RT-LAMP reaction setup**

453 Lyophilized reagents were resuspended in a final volume of 40*μ*L containing 1x
454 rehydration buffer (ThermoPol buffer (B9004S, New England Biolabs), 6mM $MgSO_4$,
455 and 0.5%*(v/v)* Triton X-100). For analytical sensitivity experiments, 2*μ*L SARS-CoV-2
456 RNA in water was added. For clinical testing, 10*μ*L extracted RNA was added to each

457 RT-LAMP reaction. For testing the contrived specimens, 10μL sample (not extracted)
458 was added to each RT-LAMP reaction. For usability testing, 40μL swab eluate was
459 added directly to the RT-LAMP reaction using transfer pipettes or the in-house unified
460 dispensers.
461
462 **Analytical sensitivity of RT-LAMP assay**
463 Analytical sensitivity of lyophilized RT-LAMP was tested using purified RNA (0-2x10^6
464 copies/40μL reaction). We also tested the effect of salt, human DNA, and mucin on
465 amplification of SARS-CoV-2 RNA and IAC DNA using simulated nasal matrix as
466 previously described(*19*).
467
468 **Preparation of contrived swab samples and kits for usability testing**
469 For the transfer pipette workflow, each kit contained one swab (either positive or
470 negative), a vial of buffer (10-500-25, Fisher Scientific, Waltham, MA) containing 400μL
471 of 1x rehydration buffer (see section RT-LAMP reaction setup) and one lyophilized RT-
472 LAMP reagent tube. For positive swabs, 10μL of 100 copies/μL SARS-CoV-2 DNA in
473 0.05% Triton X-100 was pipetted onto the swab (1804-PF, Puritan Medical) and dried at
474 room temperature in the air-clean chamber (825-PCR/HEPA, Plas-Labs, Lansing, NI)
475 for 4 hours before packaging in a sealed foil pouch with desiccant (S-8032, ULINE). The
476 unified sampler was built from parts using an assembly jig (custom order from Hygiena,
477 LLC, Camarillo, CA). The unified dispenser contained a hollow-shaft polyurethane swab
478 attached to a bulb preloaded with 400μL 1x rehydration buffer and a separate tube with

479 a filter and drip dispenser friction fit inside the tube. Each custom sampler kit contained
480 an in-house assembled dispenser unit and one lyophilized RT-LAMP reagent tube.
481
482 **Usability study**
483 The Harmony usability study was approved by the Institutional Review Board at the
484 University of Washington (IRB#: STUDY00010884), and informed consent was provided
485 by participants. HCWs (*n = 10*), including registered nurses, medical students, and
486 dental students were enrolled in this study over the course of 1 month. All data was
487 collected without identifiers. The primary objective of this study was to determine the
488 accuracy and precision of the two sample transfer methods and test if variation in
489 reproducibility impacted assay performance, and the secondary objective was to gather
490 user input on the feasibility of each protocol. Participants first received an explanation of
491 the test and its intended use, then watched an instructional video narrated by the
492 facilitator to become familiar with the Harmony workflow (**video S1 and video S2**). After
493 watching the video, participants were given a packet with a unique identifier that
494 contained comprehensive instructions for the study procedures and survey questions.
495 Study procedures were modeled on a coaching methodology(*20*), to allow natural
496 progression of the procedures and to identify blocking steps in the instructions. The
497 facilitator sat 10 feet from the participant and kept a record of verbal questions and
498 comments from participants but did not provide answers to procedural questions unless
499 the participant was could not proceed.
500

501 For part 1, data related to user preference on sample preparation, tube sizes, and their
502 level of confidence in performing each task were collected anonymously as prompts
503 within their study packet. Open-ended questions were extracted for themes in errors or
504 issues and supplemented with comments and observations recorded by the facilitator.
505 Samples were saved with deidentified labels, and after all participants had completed
506 the study facilitators measured volumes in each receiving tube from part 1. The
507 variances of the volume recovered by each method were tested for their equality using
508 F-Test, and the P-value was reported. The means of the recovered volumes transferred
509 by LPs or HCWs were compared using student's t-test (two-sided), and the P-value was
510 reported.
511
512 For part 2, each participant followed instructions in the packet and on the integrated
513 mobile phone to complete the entire Harmony workflow on four total contrived samples,
514 two samples using the transfer pipette protocol and two using the unified sampler
515 system. Kits were prepared as specified above.
516
517 The lab personnel (*n = 5*) portion of the user testing aimed to compare performance of
518 the Harmony device by HCW to that of an "experienced" population, by replicating this
519 process with four students and a researcher from the Lutz Lab. Survey questions were
520 omitted for this group because these volunteers provided feedback throughout the
521 development of Harmony and their views are included in the discussion of this

522 manuscript. The accuracies of tests performed by LPs and HCWs using each method
523 were tested for their equality using Z-test (two-sided), and the P-value was reported.
524
525 **Clinical nasal swab specimens from individuals presenting respiratory symptoms**
526 A minimum sample size of 30 (each negative and positive) was required to achieve the
527 confidence interval (**CI**) of 90 -100% (binomial cumulative distribution function) should
528 all results be accurate. Our clinical specimen panel (*n = 110*) was previously used to
529 evaluate other SARS-CoV-2 assays(*16*), but 9 specimens had insufficient volume for
530 RNA extraction and were thus excluded from the study. These specimens were
531 collected with informed consent as part of the Seattle Flu Study, approved by the
532 Institutional Review Board at the University of Washington (IRB#: STUDY0006181). All
533 participant specimens were de-identified prior to the transfer to the Lutz lab at the
534 University of Washington for analysis. The remaining 101 specimens were evaluated
535 using the newly-extracted RNA for analysis by RT-qPCR and Harmony system, to avoid
536 variations introduced from different batches of extraction. RNA was extracted
537 from clinical nasal swab specimens stored in viral transport media using
538 the QIAamp Viral RNA Mini Kit (52906; Qiagen, Hilden, Germany). Prior to extraction,
539 100μL of each specimen was mixed with 40μL negative VTM to reach the suggested
540 140μL sample volume. RNA was extracted according to the manufacturer's
541 protocol, eluted into 70μL of EB buffer, and stored at -80°C in single-use aliquots until
542 amplification. 5μL of RNA was used for analysis in 20μL RT-qPCR using U.S. CDC N1,
543 N2, or RP human control assays(*9*). 10μL of RNA was used for analysis in 40μL

544 lyophilized RT-LAMP in the Harmony workflow. Each sample was run in duplicate. Only
545 samples with positive results from both Harmony replicates were reported as positive for
546 SARS-CoV-2. Sensitivity (TP/(TP + FN)), specificity (TN/(TN+FP)), and concordance
547 ((TP+TN)/(TP+TN+FP+FN)) were calculated and reported with 95%CI using binomial
548 exact proportions.
549

550 **XPRIZE blinded contrived sample panel**

551 The blinded panel was assembled and distributed by HudsonAlpha Discovery
552 (Huntsville, AL) for COVID-19 XPRIZE competition, and information on the samples was
553 revealed to the authors only after results were submitted to XPRIZE. Samples were
554 shipped to the Lutz Lab at the University of Washington. We reported results for
555 contrived samples of chemically-inactivated SARS-CoV-2 viral particle (ZeptoMetrix
556 Corporation, Buffalo, NY) spiked in phosphate-buffered saline (**1x PBS**) (*n = 29*), nasal
557 specimens (*n = 20*), or saliva (*n = 20*) at 0 to 1000 copies/rxn. To affirm the identify of
558 these specimens, we also performed RT-qPCR using CDC primer/probes after the
559 samples had been tested using the Harmony system.
560

561 **Housing**

562 The housing combines the heater/reader assembly with the cell phone, while concealing
563 the connector cables and presenting a sturdy and easy-to-us0e platform. The 3D CAD
564 program, Fusion 360 (AutoDesk), was used for the design of housing. Prototypes were
565 printed in PLA plastic (Overture™ Filament) using a Prusa i3 MK3s at 0.3mm layer

566 height. Power was supplied to both the heater/reader assembly and the phone
567 simultaneously using the Charge-Plus USB-C (LAVA Computer Manufacturing
568 Inc.) connector device and a standard fast-charging American cellphone charger. The
569 LAVA device also facilitates the transfer of data between the devices.
570
571 **Reader/heater device**
572 The aluminum block to house the reagent tubes was custom-made by Bryan
573 Willman according to the specifications in **fig. S3**. The circuit boards were designed
574 using Autodesk Eagle (San Rafael, CA), and the assembly of the circuit boards are
575 shown in **fig. S4** and **fig. S5**. The lid, latch, and upper and lower housing of the device
576 were drawn using SolidWorks (Dassault Systèmes, Waltham, MA) and printed by
577 Xometry - HP MultiJet Fusion 3D (Gaithersburg, MD). All parts were assembled as
578 shown in **fig. S6**.
579
580 **Real-time fluorescence signal analysis**
581 After the user inserts the reaction tube into the device, the software adjusts the
582 temperature to re-equilibrate the temperature of heat block back to the reaction
583 temperature. During this initial period, the signals from the photo diodes (the blue LED
584 (FAM signal for target amplification) and the yellow LED (TEX 615 signal for the IAC
585 amplification) are collected but not used in analyses. Once the initial period is over,
586 signal analysis commences. Each signal is analyzed in real time by comparing the
587 current mean of the signal over the most recent 60s interval to the signal's behavior

588 some 360s in the past. Specifically, the current mean is compared to a bound consisting
589 of the signal's mean over the period from 420s to 360s in the past plus a multiple (1.9x
590 for target, 1.5x for IAC) of the signal's sample standard deviation over that same period.
591 If the current mean exceeds the bound, and maintains that condition for at least 15s, the
592 signal is said to have "indicated". If the signal from the target emission indicates, the
593 presence of SARS-CoV-2 has been detected, and the software immediately reports
594 "positive COVID-19". If the signal from the IAC emission indicates, successful
595 amplification of the IAC has been detected. Then, if the target emission does not also
596 indicate before the end of the run, then a "negative COVID-19" result is reported; this
597 delay in reporting negative results provides the maximum opportunity to detect low
598 concentrations of SARS-CoV-2 that may be present in samples. If neither the target
599 emission nor the IAC emission is detected, "test failed" is reported.
600
601 **REFERENCES AND NOTES**
602
603 1. World Health Organization. (2020), vol. 2021.
604 2. World Health Organization. (2021), vol. 2021.
605 3. A. Sandford. (Euronews with AP, AFP, 2020).
606 4. G. Bonaccorsi, F. Pierri, M. Cinelli, A. Flori, A. Galeazzi, F. Porcelli, A. L.
607 Schmidt, C. M. Valensise, A. Scala, W. Quattrociocchi, F. Pammolli, Economic
608 and social consequences of human mobility restrictions under COVID-19. *Proc*
609 *Natl Acad Sci U S A* **117**, 15530-15535 (2020).

610 5. I. Y. Chu, P. Alam, H. J. Larson, L. Lin, Social consequences of mass quarantine
611 during epidemics: a systematic review with implications for the COVID-19
612 response. *J Travel Med* **27**, (2020).
613 6. J. Garre-Olmo, O. Turro-Garriga, R. Marti-Lluch, L. Zacarias-Pons, L. Alves-
614 Cabratosa, D. Serrano-Sarbosa, J. Vilalta-Franch, R. Ramos, G. Girona Healthy
615 Region Study, Changes in lifestyle resulting from confinement due to COVID-19
616 and depressive symptomatology: A cross-sectional a population-based study.
617 *Compr Psychiatry* **104**, 152214 (2021).
618 7. Centers for Diseases Control and Prevention. (2021), vol. 2021.
619 8. Y. Mori, K. Nagamine, N. Tomita, T. Notomi, Detection of loop-mediated
620 isothermal amplification reaction by turbidity derived from magnesium
621 pyrophosphate formation. *Biochem Biophys Res Commun* **289**, 150-154 (2001).
622 9. U.S. Centers for Disease Control and Prevention, "CDC 2019-Novel Coronavirus
623 (2019-nCoV) Real-Time RT-PCR Diagnostic Panel For Emergency Use Only,"
624 (2020).
625 10. P. Craw, W. Balachandran, Isothermal nucleic acid amplification technologies for
626 point-of-care diagnostics: a critical review. *Lab Chip* **12**, 2469-2486 (2012).
627 11. E. Gonzalez-Gonzalez, I. M. Lara-Mayorga, I. P. Rodriguez-Sanchez, Y. S.
628 Zhang, S. O. Martinez-Chapa, G. T. Santiago, M. M. Alvarez, Colorimetric loop-
629 mediated isothermal amplification (LAMP) for cost-effective and quantitative
630 detection of SARS-CoV-2: the change in color in LAMP-based assays

631 quantitatively correlates with viral copy number. *Anal Methods* **13**, 169-178
632 (2021).
633 12. J. Rodriguez-Manzano, K. Malpartida-Cardenas, N. Moser, I. Pennisi, M. Cavuto,
634 L. Miglietta, A. Moniri, R. Penn, G. Satta, P. Randell, F. Davies, F. Bolt, W.
635 Barclay, A. Holmes, P. Georgiou, Handheld Point-of-Care System for Rapid
636 Detection of SARS-CoV-2 Extracted RNA in under 20 min. *ACS Cent Sci* **7**, 307-
637 317 (2021).
638 13. Chaibio. (Santa Clara, CA, 2021).
639 14. W. Putri, D. J. Muscatello, M. S. Stockwell, A. T. Newall, Economic burden of
640 seasonal influenza in the United States. *Vaccine* **36**, 3960-3966 (2018).
641 15. Centers for Diseases Control and Prevention. (2012).
642 16. N. Panpradist, Q. Wang, P. S. Ruth, J. H. Kotnik, A. K. Oreskovic, A. Miller, S. W.
643 A. Stewart, J. Vrana, P. D. Han, I. A. Beck, L. M. Starita, L. M. Frenkel, B. R.
644 Lutz, Simpler and faster Covid-19 testing: Strategies to streamline SARS-CoV-2
645 molecular assays. *EBioMedicine* **64**, 103236 (2021).
646 17. N. Morant, University of Bath, (2015).
647 18. Addgene. (Watertown, Massachusetts, USA, 2021), vol. 2021.
648 19. N. Panpradist, B. J. Toley, X. Zhang, S. Byrnes, J. R. Buser, J. A. Englund, B. R.
649 Lutz, Swab sample transfer for point-of-care diagnostics: characterization of
650 swab types and manual agitation methods. *PLoS One* **9**, e105786 (2014).
651 20. R. Mack, J. B. Robinson, in *The Psychology of Expertise,* H. R.R., Ed. (Springer,
652 New York, NY, 1992), pp. 245-268.

653 21. FPbase. (2021), vol. 2020.

654 22. Newport. (2021), vol. 2021.

655 23. Mousers Electronics. (2021), vol. 2021.

656 24. A. Alekseenko, D. Barrett, Y. Pareja-Sanchez, R. J. Howard, E. Strandback, H.
657 Ampah-Korsah, U. Rovsnik, S. Zuniga-Veliz, A. Klenov, J. Malloo, S. Ye, X. Liu,
658 B. Reinius, S. J. Elsasser, T. Nyman, G. Sandh, X. Yin, V. Pelechano, Direct
659 detection of SARS-CoV-2 using non-commercial RT-LAMP reagents on heat-
660 inactivated samples. *Sci Rep* **11**, 1820 (2021).

661 25. B. A. Rabe, C. Cepko, SARS-CoV-2 detection using isothermal amplification and
662 a rapid, inexpensive protocol for sample inactivation and purification. *Proc Natl*
663 *Acad Sci U S A* **117**, 24450-24458 (2020).

664 26. S. Wei, E. Kohl, A. Djandji, S. Morgan, S. Whittier, M. Mansukhani, E. Hod, M.
665 D'Alton, Y. Suh, Z. Williams, Direct diagnostic testing of SARS-CoV-2 without the
666 need for prior RNA extraction. *Sci Rep* **11**, 2402 (2021).

667 27. V. L. Dao Thi, K. Herbst, K. Boerner, M. Meurer, L. P. Kremer, D. Kirrmaier, A.
668 Freistaedter, D. Papagiannidis, C. Galmozzi, M. L. Stanifer, S. Boulant, S. Klein,
669 P. Chlanda, D. Khalid, I. Barreto Miranda, P. Schnitzler, H. G. Krausslich, M.
670 Knop, S. Anders, A colorimetric RT-LAMP assay and LAMP-sequencing for
671 detecting SARS-CoV-2 RNA in clinical samples. *Sci Transl Med* **12**, (2020).

672 28. L. Bokelmann, O. Nickel, T. Maricic, S. Paabo, M. Meyer, S. Borte, S.
673 Riesenberg, Point-of-care bulk testing for SARS-CoV-2 by combining

674 hybridization capture with improved colorimetric LAMP. *Nat Commun* **12**, 1467
675 (2021).
676 29. W. Yamazaki, Y. Matsumura, U. Thongchankaew-Seo, Y. Yamazaki, M. Nagao,
677 Development of a point-of-care test to detect SARS-CoV-2 from saliva which
678 combines a simple RNA extraction method with colorimetric reverse transcription
679 loop-mediated isothermal amplification detection. *J Clin Virol* **136**, 104760
680 (2021).
681 30. J. Qian, S. A. Boswell, C. Chidley, Z. X. Lu, M. E. Pettit, B. L. Gaudio, J. M.
682 Fajnzylber, R. T. Ingram, R. H. Ward, J. Z. Li, M. Springer, An enhanced
683 isothermal amplification assay for viral detection. *Nat Commun* **11**, 5920 (2020).
684 31. M. Patchsung, K. Jantarug, A. Pattama, K. Aphicho, S. Suraritdechachai, P.
685 Meesawat, K. Sappakhaw, N. Leelahakorn, T. Ruenkam, T. Wongsatit, N.
686 Athipanyasilp, B. Eiamthong, B. Lakkanasirorat, T. Phoodokmai, N. Niljianskul,
687 D. Pakotiprapha, S. Chanarat, A. Homchan, R. Tinikul, P. Kamutira, K.
688 Phiwkaow, S. Soithongcharoen, C. Kantiwiriyawanitch, V. Pongsupasa, D.
689 Trisrivirat, J. Jaroensuk, T. Wongnate, S. Maenpuen, P. Chaiyen, S.
690 Kamnerdnakta, J. Swangsri, S. Chuthapisith, Y. Sirivatanauksorn, C. Chaimayo,
691 R. Sutthent, W. Kantakamalakul, J. Joung, A. Ladha, X. Jin, J. S. Gootenberg, O.
692 O. Abudayyeh, F. Zhang, N. Horthongkham, C. Uttamapinant, Clinical validation
693 of a Cas13-based assay for the detection of SARS-CoV-2 RNA. *Nat Biomed Eng*
694 **4**, 1140-1149 (2020).

32. J. Joung, A. Ladha, M. Saito, M. Segel, R. Bruneau, M. W. Huang, N. G. Kim, X. Yu, J. Li, B. D. Walker, A. L. Greninger, K. R. Jerome, J. S. Gootenberg, O. O. Abudayyeh, F. Zhang, Point-of-care testing for COVID-19 using SHERLOCK diagnostics. *medRxiv*, (2020).

33. J. P. Broughton, X. Deng, G. Yu, C. L. Fasching, V. Servellita, J. Singh, X. Miao, J. A. Streithorst, A. Granados, A. Sotomayor-Gonzalez, K. Zorn, A. Gopez, E. Hsu, W. Gu, S. Miller, C. Y. Pan, H. Guevara, D. A. Wadford, J. S. Chen, C. Y. Chiu, CRISPR-Cas12-based detection of SARS-CoV-2. *Nat Biotechnol* **38**, 870-874 (2020).

ACKNOWLEDGMENTS

We thank Bryan Willman for his support in fabricating customized heat blocks, Jan Gray for his help with firmware development, Tom Blank for sharing the PCB fabrication resources, and Dr. Liz Sanocki for the useful feedback on the software user interface. We thank Shawna Cooper for sharing the graphics and content used in Audere's mobile app's flu@home, which influenced the design of the first few screens of the Harmony COVID-19 software. We thank Dr. Paul Yager and Steven Bennett for use of their optical filters during the initial stage of device development. We thank Jason Tauscher at the Washington Nanofabrication Facility for his assistance in cutting the plastic sheet filters. The Washington Nanofabrication Facility is a National Nanotechnology Coordinated Infrastructure (NNCI) site at the University of Washington with partial support from the National Science Foundation via awards NNCI-2025489 and NNCI-

717 1542101. We thank Seattle Flu Study researchers Dr. Jay Shendure and Dr. Jase
718 Gehring for their helpful technical discussion. We thank Dr. Syamal Raychaudhuri, Dr.
719 Frances Chu from Inbios International, and Dr. Gwong-Jen J. Chang for the stimulating
720 discussion. We thank the Seattle Flu Study and the Seattle Coronavirus Assessment
721 Network (SCAN) teams led by Principal Investigators: Helen Y. Chu, MD, MPH, Michael
722 Boeckh, MD, PhD, Janet A. Englund, MD, Michael Famulare, PhD, Barry R. Lutz, PhD,
723 Deborah A. Nickerson, PhD, Mark J. Rieder, PhD, Lea M. Starita, PhD, Mathew
724 Thompson, MD, MPH, DPhil, Jay Shendure, MD, PhD and Trevor Bedford, PhD for
725 providing specimens for testing. **Funding**: This work was supported by the Seattle Flu
726 Study (funded by Gates Ventures) and the National Institutes of Health (R01AI140845;
727 5R61AI140460-03). We thank the Washington Entrepreneurial Research Evaluation
728 and Commercialization HUB program (WE-REACH, U01 HL152401) and their matching
729 grant partners for partly supporting reagents, supplies, and personnel. I.T.H. was
730 supported in part by the National Institute of General Medical Sciences of the National
731 Institutes of Health under Award Number T32GM008268. This work does not reflect the
732 views of the funders. The funders were not involved in the design of the study, and
733 funders do not have any ownership over the management and conduct of the study, the
734 data, or the rights to publish. **Author contributions:** N.P. developed lyophilized RT-
735 LAMP and outlined the overall plan for experiments and data visualization presented in
736 this manuscript. R.G.A. developed a mobile software application for operating the
737 device and analyzing results in real-time. M.R. developed the heater and fluorescent
738 reader device. E.K. designed the RT-LAMP assay primers and probes and engineered

739 polymerase. E.K., I.T.H., and Q.W. synthesized polymerase and provided usability
740 feedback during the development of the Harmony COVID-19 system. I.T.H. and Q.W.
741 prepared *in vitro* RNA transcripts. J.H.K. and V.L. led the usability study. N.P., A.K.O.,
742 and C.B. tested clinical and contrived specimens. R.G.A., N.P., A.K.O., and J.H.K.
743 analyzed the data. I.T.H. and Q.W. prepared the kits and blinded mock samples for
744 usability testing. D.L. developed housing units to integrate the cell phone, sample
745 preparation station, and the device. L.M.S. and P.D.H. designed and characterized the
746 clinical specimen panel used in this study. M.T. oversaw the usability study. B.R.L.
747 oversaw the development and evaluation of the Harmony COVID-19 system. All authors
748 contributed to writing this manuscript and approved the final version. **Competing**
749 **interest:** Provisional patent applications have been filed on several components of the
750 Harmony COVID-19 system. N.P., R.G.A., M.R., E.K., Q.W., I.T.H., D.L., and B.R.L. are
751 inventors on one or more provisional patent applications. N.P., R.G.A., M.R., E.K.,
752 Q.W., I.T.H., J.H.K., A.K.O., C.B., D.L., and B.R.L. anticipate forthcoming equity in a
753 startup company that has licensed related technology and supports ongoing work in the
754 B.R.L. laboratory at the University of Washington but played no role in the study. M.T. is
755 on the Advisory Board for Visby Medical which produces tests for COVID-19 and has
756 received reimbursement for this work. He has also received reimbursement for medical
757 advice to Roche Molecular Diagnostics and Inflammatix. **Data and materials**
758 **availability:** All data are presented in the main text and supplementary information.
759 **Code availability:** Sequence alignment and primer design was performed using
760 Geneious 8.1.9 (Auckland, New Zealand). CFX-Maestro (BioRad, Hercules, CA) was

761 used to analyze the RT-PCR results. TapeStation Software (Agilent, Santa Clara, CA)
762 was used to visualize fragments of synthetic RNA. A provisional patent application was
763 filed regarding aspects of the cell phone application. The data analysis algorithm is
764 described in the manuscript.
765
766 **FIGURE CAPTIONS:**
767

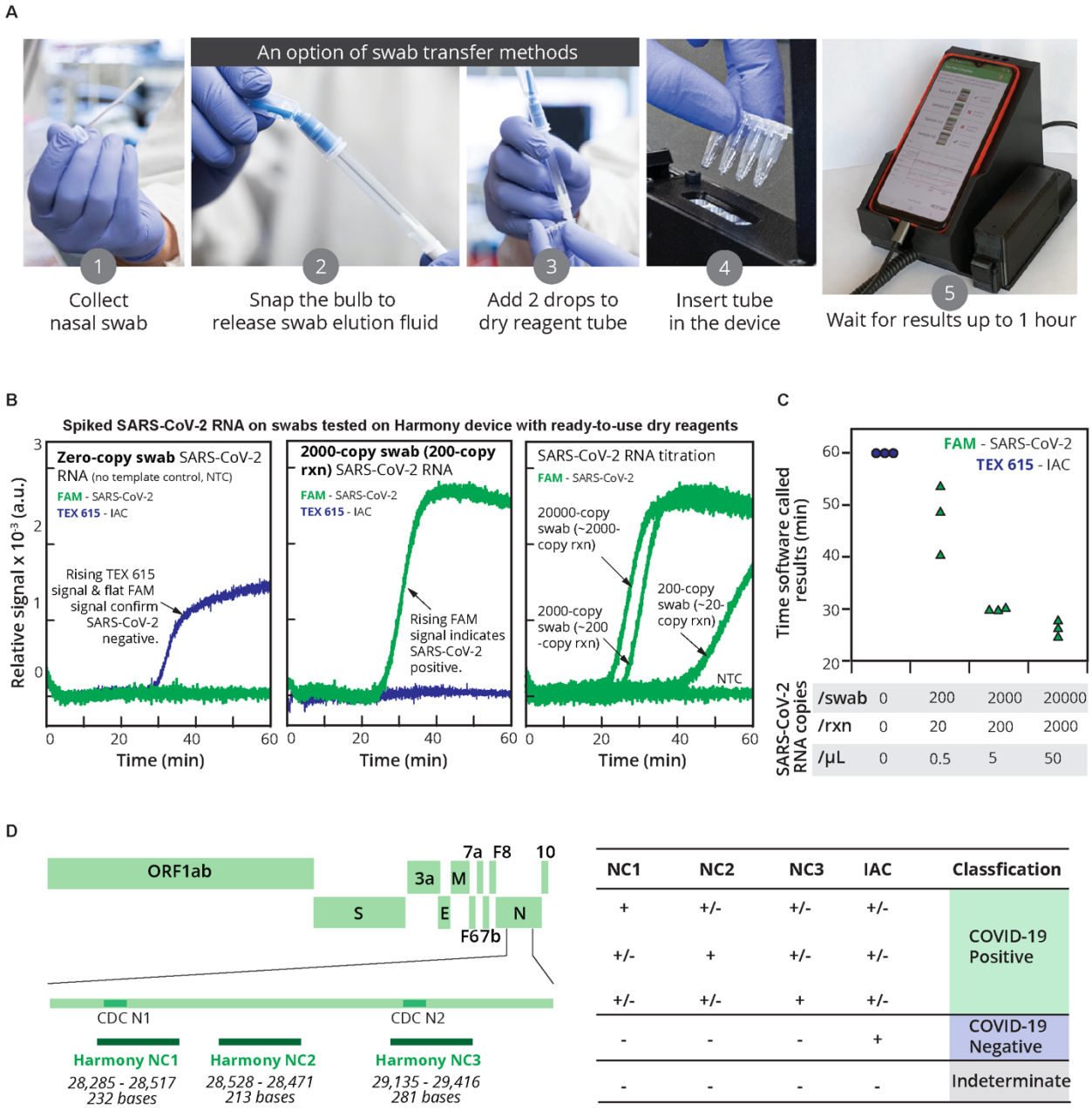

Fig. 1 Harmony COVID-19 workflow, analytical performance, and interpretation. (**A**) User workflow. A nasal swab is collected and eluted in the rehydration buffer using either a unified sampler-dispenser (shown) or a tube-and-bulb method (**Fig. 6**). The swab eluate is then transferred into the reaction tube to rehydrate lyophilized, pre-loaded RT-LAMP reagents. Users follow the instructions on the cell phone app to record

774 the sample identity, insert the tube in the test slot, and close the device. Four samples
775 can be analyzed in parallel. (Photo credits: a1-a4, Mark Stone at the University of
776 Washington and a5, Christopher Snyder at North Seattle College). (**B**) Examples of on-
777 device analysis. Lyophilized reagents were rehydrated with the eluate from swabs
778 spiked with 0, 200, 2000, or 20,000 copies of SARS-CoV-2 RNA, run on the device, and
779 analyzed in real time. The samples with SARS-CoV-2 RNA at 2000, 200, and 20
780 copies/reaction (**rxn**) were reported as positive by software at 27 min, 30 min, and 41
781 min, respectively; after 60 min the NTC reaction was classified as negative. (**C**) Time-to-
782 result. Individual detection time points (*n = 3*) are plotted. Variation in detection time
783 increases as samples approach the detection limit. (**D**) Diagnostic algorithm. Harmony
784 COVID-19 software calls samples as positive, negative, or indeterminate based on
785 detection of the three regions in nucleocapsid gene (NC1 overlapping with the CDC N1
786 region, NC2, and NC3 overlapping with the CDC N2 region) and the engineered IAC
787 sequence.
788
789

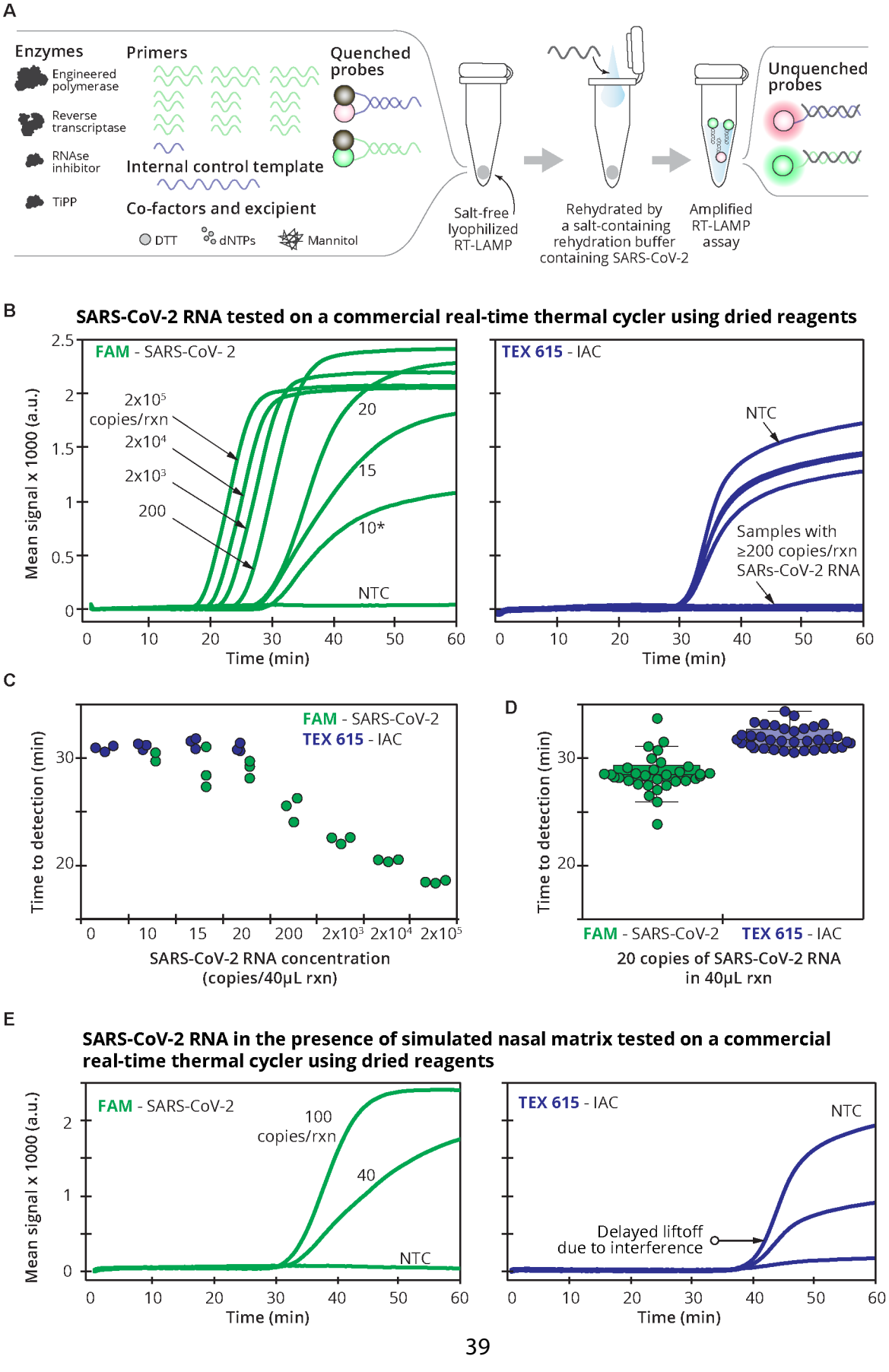
A
Enzymes
Engineered polymerase
Reverse transcriptase
RNAse inhibitor
TiPP
Primers
Internal control template
Co-factors and excipient
DTT
dNTPs
Mannitol
Quenched probes
Salt-free lyophilized RT-LAMP
Rehydrated by a salt-containing rehydration buffer containing SARS-CoV-2
Amplified RT-LAMP assay
Unquenched probes
B
SARS-CoV-2 RNA tested on a commercial real-time thermal cycler using dried reagents
FAM - SARS-CoV- 2
2x10⁵ copies/rxn
2x10⁴
2x10³
200
20
15
10*
NTC
Mean signal x 1000 (a.u.)
Time (min)
TEX 615 - IAC
NTC
Samples with ≥200 copies/rxn SARs-CoV-2 RNA
C
FAM - SARS-CoV-2
TEX 615 - IAC
Time to detection (min)
SARS-CoV-2 RNA concentration (copies/40µL rxn)
D
FAM - SARS-CoV-2
TEX 615 - IAC
20 copies of SARS-CoV-2 RNA in 40µL rxn
E
SARS-CoV-2 RNA in the presence of simulated nasal matrix tested on a commercial real-time thermal cycler using dried reagents
FAM - SARS-CoV-2
100 copies/rxn
40
NTC
TEX 615 - IAC
NTC
Delayed liftoff due to interference

790

791

792 **Fig. 2 Lyophilized RT-LAMP and its analytical sensitivity.**

793 (**A**) To set up the assay, a sample in elution/rehydration buffer containing
794 magnesium, Thermopol buffer, and detergents is added to rehydrate the lyophilized RT-
795 LAMP reagents in a single step. (**B**) Real-time amplification signal of RT-LAMP
796 reactions containing SARS-CoV-2 RNA (**NTC**; no template control), 10, 15, 20, 200,
797 2000, $2x10^4$, or $2x10^5$ copies/40μL reaction (**rxn**). The left panel shows the average (*n =*
798 *3*) FAM signal detecting SARS-CoV-2. *Only 2/3 replicates of 10 copies/rxn amplified so
799 the average was from duplicate reactions. The right panel shows TEX 615 signal
800 detecting the internal amplification control (IAC). The IAC was detected in the NTC (*n =*
801 3) and in the single 10 copies/rxn that did not detect SARS-CoV-2. (**C**) Time to detection
802 of SARS-CoV-2 and IAC targets reported by the real-time thermal cycler. Individual data
803 points are plotted. Note that only 2/3 replicates of 10 copies/rxn amplified. IAC signals
804 were properly detected in NTC (*n = 3*) and 1 of the 3 replicates of 10 copies/rxn
805 undetected for SARS-CoV-2. (**D**) Evaluation of analytical sensitivity at 20 copies/rxn of
806 SARS-CoV-2 RNA (*n = 40*), performed in two different runs (*n = 20* each) with two
807 different serially diluted RNA samples. Time-to-result of individual samples are plotted
808 along with medians (middle lines of the boxes), interquartile ranges (edges of the
809 boxes), ranges (the ends of whiskers), and outliers (data points outside the whiskers).
810 (**E**) Impact of nasal matrix. SARS-CoV-2 RNA at 0, 40, or 100 copies/rxn was amplified
811 in lyophilized RT-LAMP in the presence of simulated nasal matrix (*n = 3*). All data was

812 measured every 13s using FAM and TEX 615 channels, by a real-time thermal cycler in

813 1h reactions at 63.3°C, and (**C**).

814

815

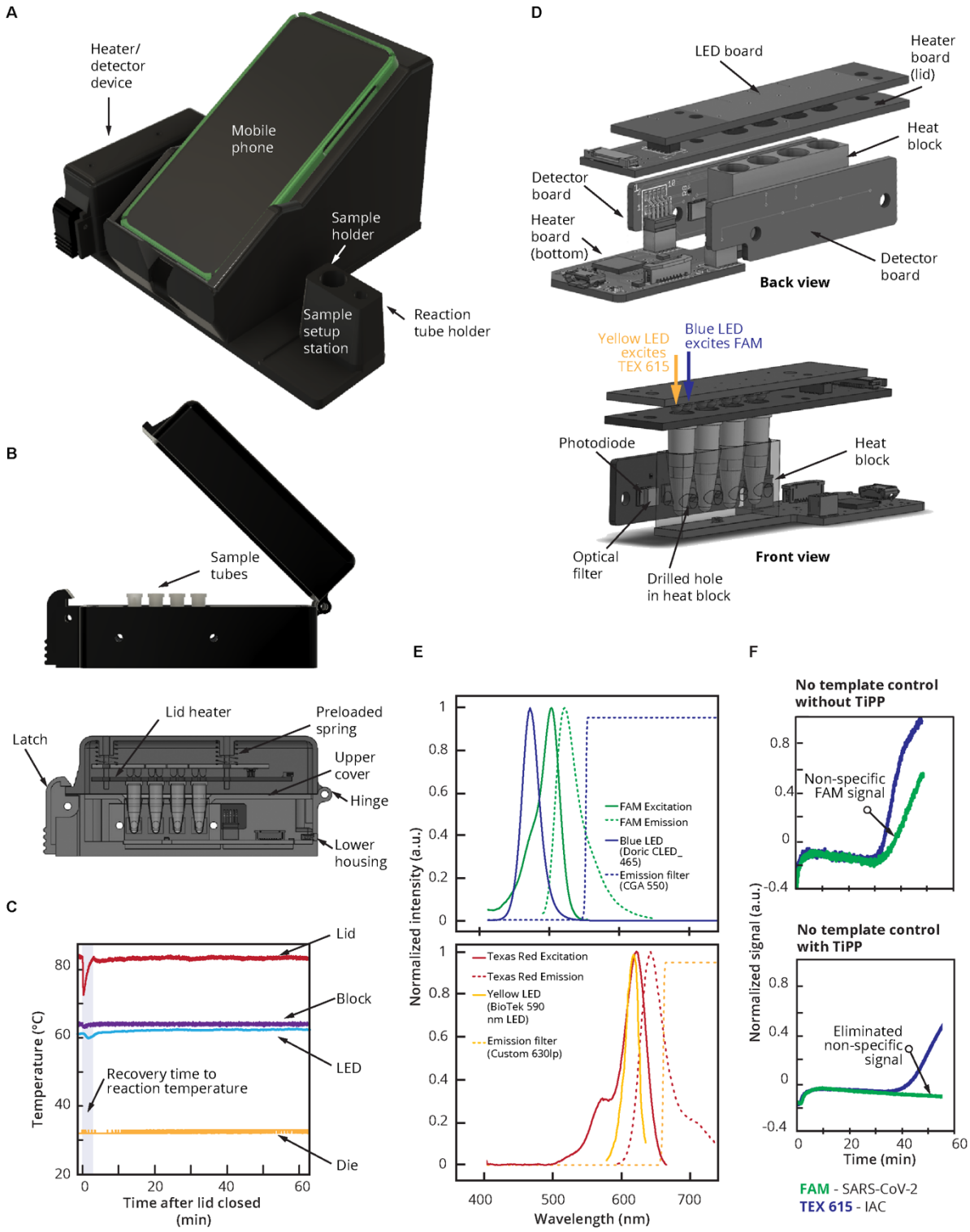

Fig.3 Overview of Harmony COVID-19 hardware.

819 (**A**) Plastic case cradles the cell phone (removable and connected by a spring cable),
820 mounts the heater/reader device, and houses a Charge-Plus USB-C connector hub (not
821 shown). A sample station holds the sample and reaction tube during processing and is
822 detachable to allow cleaning. Weight: 266g housing, 104g heater/reader device (total
823 <0.5kg). Dimensions: 205mm x 167.5mm x 125mm housing, 30mm x 120mm x 50mm
824 heater/reader device. (**B**) The heater/reader device contains an aluminum block with
825 wells for four samples (0.2mL reagent tubes) and is heated from the bottom by a
826 resistive heater made from serpentine conductive traces on a printed circuit board. In
827 the middle of the heater, a temperature sensor (Class B Platinum RTD) is used to
828 measure the heat block temperature. Power to the heater is supplied by a MOSFET and
829 modulated by varying the PWM duty cycle of the MOSFET. (**C**) Temperature profile
830 after the lid opening throughout a 60-min assay run. The microcontroller
831 (die) is measured to ensure the electronics are not overheated. (**D**) Lid heater, LED, and
832 detector. A heater (85°C) on top of the tube prevents condensation on the tube lid. The
833 lid heater is spring loaded to apply a preload force to the tubes to ensure good thermal
834 contact and contains pass-through holes for excitation LEDs. (**E**) Spectral
835 characteristics of the detection system. Blue and yellow LEDs provide excitation for
836 FAM and TEX 615, respectively, and photodetectors on each side detect light passing
837 through emission filters (spectral information from manufacturers(*21-23*)). The LEDs are
838 operated independently (only one LED is illuminated at a given time). (**F**) Effect of
839 thermostable inorganic pyrophosphatase (**TiPP**) on RT-LAMP signal in the Harmony

device. Normalized signal of negative control samples using the RT-LAMP formulation with and without TiPP (*n = 1* each) at 64°C.

Fig. 4 Cell phone user interface and result reporting.

The Android Harmony application guides the user through steps to set up and run the test. (**A**) Intended use of the device. (**B**) Instructions for the user to prepare samples. (**B**) Selection of the number of samples. (**D**) Collection of sample identifiers by barcode, photo capture, or manual typing. (**E**) Instruction to insert the tube when the temperature of the device reaches the reaction temperature. (**F**) Real-time analysis during the test run. (**G**) Positive results are reported as soon as they are detected. (**H**) Negative and IND results are reported at the end of the run time.

A

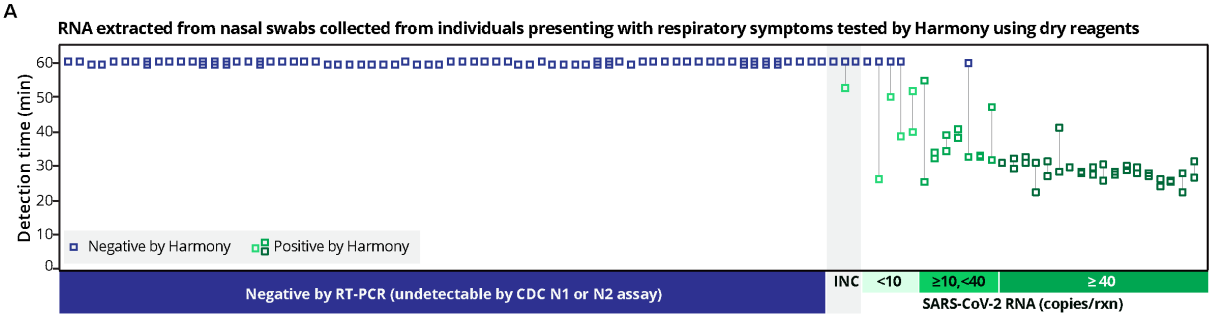

B

RNA extracted from nasal swabs collected from SARS-CoV-2 negative individuals presenting respiratory symptoms tested on Harmony device using dry reagents

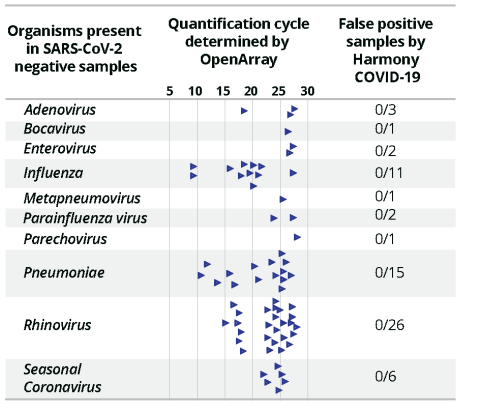

D

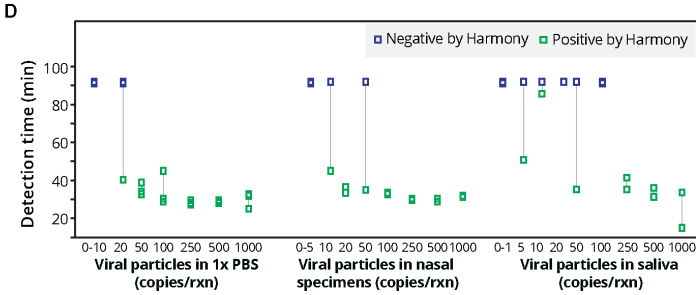

Zeptometrix viral particles (copies/rxn)	Viral particles in 1x PBS (copies/rxn)	Viral particles in nasal specimens (copies/rxn)	Viral particles in saliva (copies/rxn)
0	0/2	0/2	0/2
1	0/3	0/2	0/2
5	0/3	0/2	1/2
10	0/3	1/2	1/2
20	1/3	2/2	0/2
50	3/3	1/2	1/2
100	3/3	2/2	0/2
250	3/3	2/2	2/2
500	3/3	2/2	2/2
1000	3/3	2/2	2/2

C

Thresholds of SARS-CoV-2 RNA in positive clinical specimens (copies/rxn)	TP	TN	FP	FN	Sensitivity	Specificity
> 0	25	68	0	5	83%	100%
≥ 10	24	68	0	1	96%	100%
≥ 40	18	68	0	0	100%	100%

E

Thresholds of Zeptometrix viral particles (copies/rxn)	Matrix	TP	TN	FP	FN	Sensitivity	Specificity
≥ 20	1x PBS	16	2	0	2	89%	100%
≥ 50		12	2	0	0	100%	100%
≥ 20	Nasal matrix	11	2	0	1	92%	100%
≥ 100		8	2	0	0	100%	100%
≥ 20	Saliva	7	2	0	5	58%	100%
≥ 250		6	2	0	0	100%	100%

Fig. 5 Harmony COVID-19 performance on clinical and blinded contrived specimens.

(**A**) Detection time called by Harmony COVID-19 software for the analysis of purified RNA extracted from human nasal specimens from 101 patients presenting respiratory symptoms. Stored specimens were re-tested by RT-qPCR using N1 and N2 CDC primers; results matched previous results in 30 previous positive specimens (positive for N1 and N2) and 68 previous negative specimens, with three previous positive

862 specimens classified as inconclusive (INC) because they were negative for either CDC
863 N1 or CDC N2 by RT-qPCR. Samples are ranked from left to right by increasing SARS-
864 CoV-2 concentrations as determined by RT-qPCR. Extracted RNA from specimens was
865 analyzed by Harmony COVID-19 (10μL RNA in 40μL RT-LAMP dry reagents, *n = 2*).
866 Samples were classified as positive by Harmony only if both replicates were detected.
867 The classification results by Harmony were compared to RT-qPCR using CDC primers
868 and probes (5μL RNA in 20μL RT-qPCR reaction). (**B**) Organisms in clinical samples
869 collected from individuals presenting with respiratory symptoms were quantified using
870 OpenArray, as previously described(*16*). High quantification cycle values indicate low
871 concentrations. All these specimens were correctly identified as SARS-CoV-2 negative
872 by Harmony. (**C**) Summary table for the sensitivity and specificity of the Harmony
873 COVID-19 system using extracted RNA from clinical specimens (RT-qPCR INC
874 samples excluded). (**D**) Blinded analysis of XPRIZE contrived sample panel. The assay
875 was run for 90 min (30 min longer than **Fig. 5A** to accommodate inhibitors that may be
876 present in these blinded samples). The table below shows the detectable samples over
877 the total number of tested technical replicates. (**E**) Summary table for the sensitivity and
878 specificity of the Harmony COVID-19 system on the XPRIZE contrived samples.
879
880

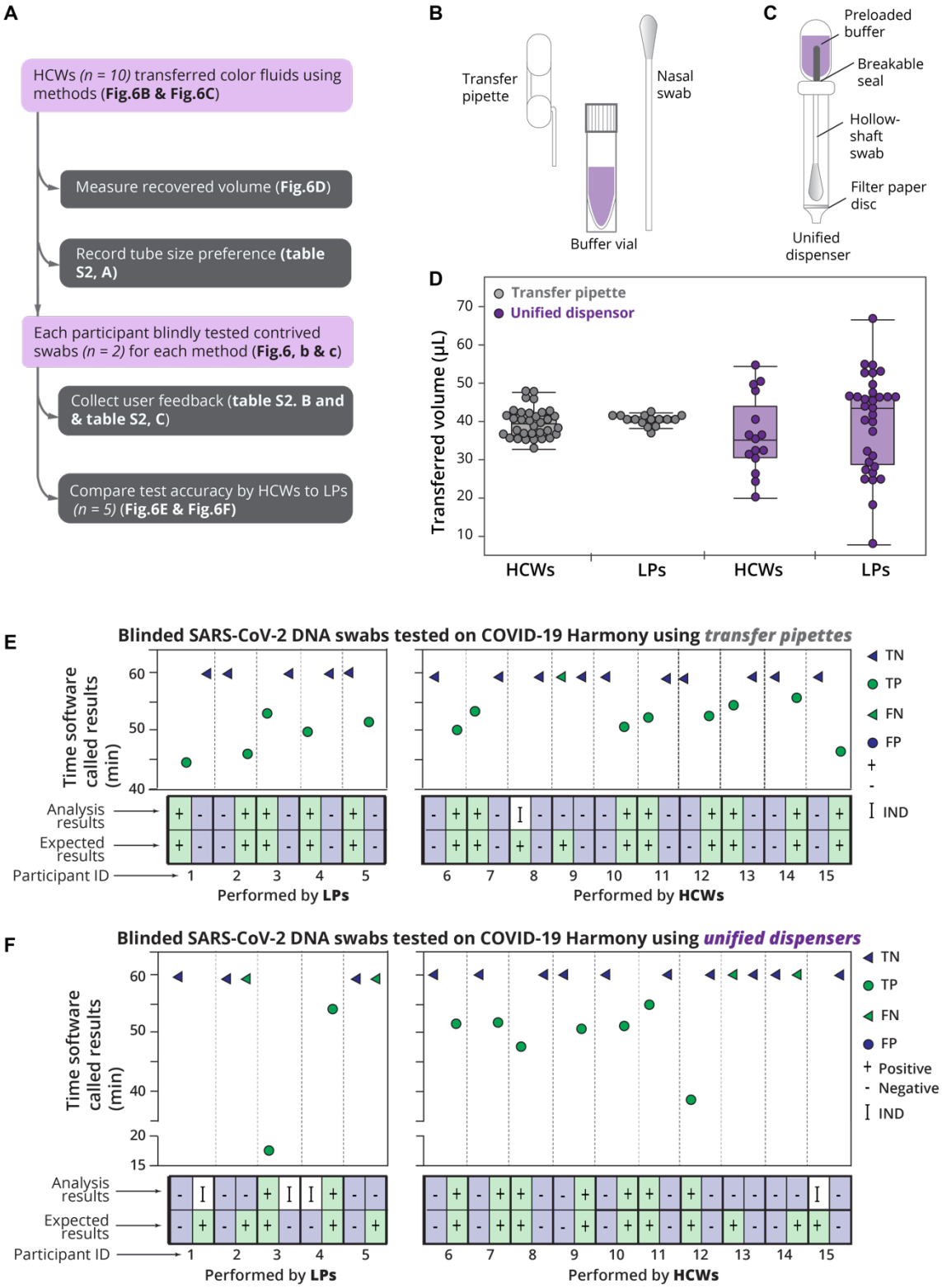

G

	Performance with *transfer pipettes*						
	TP	TN	FP	FN	IND	% Accuracy	% IND
LPs	5	5	0	0	0	100	0
HCWs	9	9	0	1	1	95	5

H

Performance with *unified dispenser*						
TP	TN	FP	FN	IND	% Accuracy	% IND
2	3	0	2	3	71	30
7	10	0	2	1	89	5

881

882

883 **Fig. 6 Usability study of Harmony COVID-19 workflow including two sample**

884 **transfer methods at the POC**.

885 (**A**) Study design. (**B**) Illustration of the first sample transfer method including a

886 volumetric transfer pipette (40μL), a nasal swab, and a pre-loaded buffer vial. **video S1**

887 demonstrates this workflow. Briefly, swabs are manually rubbed on the side of the tube

888 for 30 seconds, soaked for 1 minute, and removed. The pipette is then used to transfer

889 the swab eluate to rehydrate the lyophilized RT-LAMP reaction tube. (**C**) Illustration of

890 the second sample transfer method option using a unified dispenser, which integrates a

891 swab, buffer container, and a dropper in a single device. The contained buffer is

892 released to elute the swab sample by cracking a conduit, the user agitates the fluid by

893 shaking the tube, and a dropper tip allows the use to transfer two drops of fluid to the

894 reaction tube by squeezing the body of the device. **video S2** demonstrates this

895 workflow. (**D**) Volume transferred by each method performed by healthcare workers

896 (**HCWs**) or laboratory personnel (**LPs**). Individual volume measurements are plotted

897 along with medians (middle lines of the boxes), interquartile ranges (edges of the

898 boxes), and ranges (the ends of whiskers). **e** and **f**, Assay performance on blinded

899 contrived swabs (one negative swab and one positive swab with SARS-CoV-2 DNA at

900 1,000 copies/swab, corresponding to 100 copies/rxn) by LPs (*n = 5*) and untrained

901 HCWs (*n = 10*) using transfer pipettes, (**E**) or unified dispensers, (**F**) The usability

902 experiment written protocol is available on protocol.io

903 (https://dx.doi.org/10.17504/protocols.io.bkvskw6e) and as a visual demonstration in

904 **video S1 and video S2**. (**G**) Performance summary for the transfer pipette method. (**H**)
905 Performance summary for the unified dispenser method.
906
907 **TABLE CAPTIONS:**
908 **Table 1** Feature comparison between the Harmony COVID-19 system and other
909 assays. (**A**) Comparison to the U.S. CDC assay.(*9*) Full cost calculations for reagents
910 and devices are enclosed in **tables S3** and **table S4**.
911

Item	Standard RT-PCR assay (based on the U.S. CDC protocol)(*9*)	Covid-19 Harmony
SARS-CoV-2 primer detection	Separate reactions for N1 and N2	Multi-target redundancy amplifying three regions of the N gene in a single reaction tube
Process control	Human RP gene	Engineered internal control
LoD	1-3.2 copies/μL from extracted RNA	0.5 copies/μL (20 copies/40μL rxn) from synthetic RNA; 1 copies/μL (40 copies/40μL rxn) from extracted RNA from VTM; 2.5 copies/μL (100 copies/40μL rxn) from contrived nasal samples
Consumable cost	$12.94 ($6 extraction kit and $6.94 for RT-PCR Taq Path/IDT probes)	$8.00
Easy to use reagents	No	Yes
Batch size	24 specimens	Not required, run up to 4 samples
Equipment cost	> $5000 qPCR machine	$247 customized heater/reader
Time for sample-to-result	260 min	21-91 min

	Hands-on: 120 min Wait-time: 120 min Interpretation: 20 min	Hands-on: 1 min for direct amplification Wait-time: 20-45 min for positive samples, but 90 min is required to confirm true negative

912 (**B**) Comparison of Harmony COVID-19 to other isothermal assays for SARS-CoV-2.

Published assays	Amplification chemistry	Multi-target redundancy in a single tube	Reported LoD	User-friendly devices with ready-to-use reagents and a closed system	Demonstration of use by HCWs
Harmony COVID-19 (This study)	RT-LAMP	Yes	0.5-2.5 copies/μL	Yes	Yes
A Alekseenko *et. al.* 2021(*24*)	RT-LAMP	No	10 copies/μL	No	No
BA Rabe and C Cepko(*25*)	RT-LAMP	No	50 copies/μL	No	No
S Wei, *et. al.*(*26*)	RT-LAMP	No	2.5 copies/μL	No	No
D Thi, *et. al.* (*27*)	RT-LAMP	No	5 copies/μL	No	No
L Bokelmann *et. al.* (*28*)	RT-LAMP	No	5-20 copies/μL	No	No
W Yamaziki *et. al.* (*29*)	RT-LAMP	Yes	25 copies/μL	No	No
J Qian *et. al.*(*30*)	RPA	Yes	0.5 copies/μL	No	No

M Patchsung *et. al.*(*31*)	SHERLOCK	No	2.1 copies/μL	No	No
J Joung *et. al.*(*32*)	SHERLOCK	No	2 copies/μL	No	No
J Broughton *et.al.* (*33*)	CRISPR cas12	No	10 copy/μL	No	No

913

914

915 **SUPPLEMENTARY INFORMATION:**

916 **fig. S1** Effects of excipients on fresh RT-LAMP reactions tested on a commercial real-
917 time thermal cycler.

918 **fig. S2** Cross-reactivity of MERS and SARS in lyophilized RT-LAMP.

919 **fig. S3** Heat block used in Harmony COVID-19 device.

920 **fig. S4** The design of optical and heater circuit boards for the Harmony COVID-19
921 device.

922 **fig. S5** Circuit board assembly and required parts

923 **fig. S6** Device assembly

924 **video S1** Demonstration of transfer pipette workflow incorporated with Harmony
925 COVID-19.

926 **video S2** Demonstration of the integrated sampling system workflow with Harmony
927 COVID-19

928 **table S1** Primers, probes, and control sequences.

929 **table S2** Feedback from the HCWs

930 **table S3** Detailed reagent and device cost at a production scale of 10,000 units.

931 **table S4** Consumable costs per test

932

933 **SUPPLEMENTARY INFORMATION**

934 Trehalose can stabilize several enzymes, but we found that 2.5% (*w/v*) trehalose

935 resulted in a slower reaction at 63°C, the optimal reaction temperature of the excipient-

936 free RT-LAMP. An increase of reaction temperature to 65°C can speed up the

937 trehalose-containing RT-LAMP reactions but resulted in unreliable detection at 20 RNA

938 copies/reaction (**fig. S1**).

A

Target (copies/ reaction)	min to detection							
	65 °C		63 °C		59 °C		55 °C	
	SARS-CoV-2	IAC	SARS-CoV-2	IAC	SARS-CoV-2	IAC	SARS-CoV-2	IAC
0	N/A	27.3, 27.7	N/A	31.8, 30.7	N/A	44.7, 42.6	N/A	N/A
20	N/A	29.8, 27.5	N/A, 31.63	30.6, 32.1	N/A, 43.0	42.0, 42.8	N/A	N/A, 60.4
200	N/A	27.3, 27.4	N/A, 27.86	29.4, 39.5	N/A, 43.2	47.9, 40.4	N/A	N/A, 62.0
2000	24.7, 28.6	N/A	28.0, 28.2	30.3, 32.8	N/A, 51.0	43.3, 41.8	N/A	N/A, 60.3

B

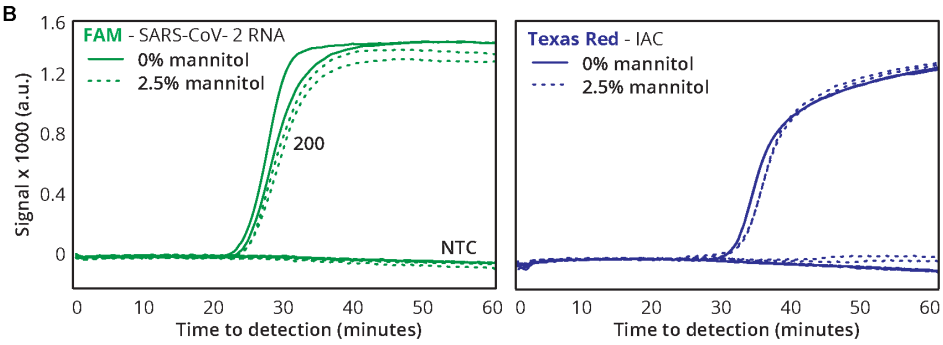

% mannitol	Target (copies/reaction)	SARS-CoV-2 (min to detection)	IAC (min to detection)
0	0	N/A	33.0, 33.0
	20	25.0, 25.7	N/A
2.5	0	N/A	33.9, 34.0
	20	26.3, 26.3	N/A

939

940

941 **fig. S1 Effects of excipients on fresh RT-LAMP reactions tested on a commercial**
942 **real-time thermal cycler.** (**A**) Time to detection of SARS-CoV-2 RNA and IAC targets
943 in the RT-LAMP containing 2.5% *(w/v)* trehalose and 0-2000 copies of SARS-CoV-2
944 RNA/40μL reaction. N/A means undetectable. For each condition, two technical
945 replicates were run at 4 different reaction temperatures (i.e., 55°C, 59°C, 63°C, and
946 65°C). (**B**) Time to detection of SARS-CoV-2 RNA and IAC targets in the RT-LAMP
947 reactions containing 0 or 20 copies of SARS-CoV-2 RNA/reaction, with and without
948 2.5% (*w/v*) mannitol, at 63°C.
949

non-SARS-CoV-2 RNA (copies/reaction)	SARS-CoV-2 RNA (copies/reaction)	min to detection SARS-CoV-2	IAC
4000 copies SARS-CoV-1	0	N/A	29.0, 30
4000 copies SARS-CoV-1	100	23.5, 24.1	N/A
4000 copies MERS	0	N/A	29.8, 30.1
4000 copies MERS	100	24.7, 24.7	N/A

950
951
952 **fig.S2 Cross-reactivity of MERS and SARS in lyophilized RT-LAMP.**
953 Detection time (min) of SARS-CoV-2 RNA and IAC targets in the presence of 4000
954 copies of either SARS-CoV-1 RNA or MERS RNA in 40μL RT-LAMP reactions at 63°C.
955 Two technical replicates were conducted in each condition. In the reactions without
956 SARS-CoV-2 RNA, we did not observe amplification of FAM signal but observed IAC
957 amplification indicating the amplification reaction was functioning properly in each
958 replicate. 100 copies of SARS-CoV-2 RNA were amplified in each positive control
959 replicate, indicating proper function of SARS-CoV-2 amplification in this master mix.
960

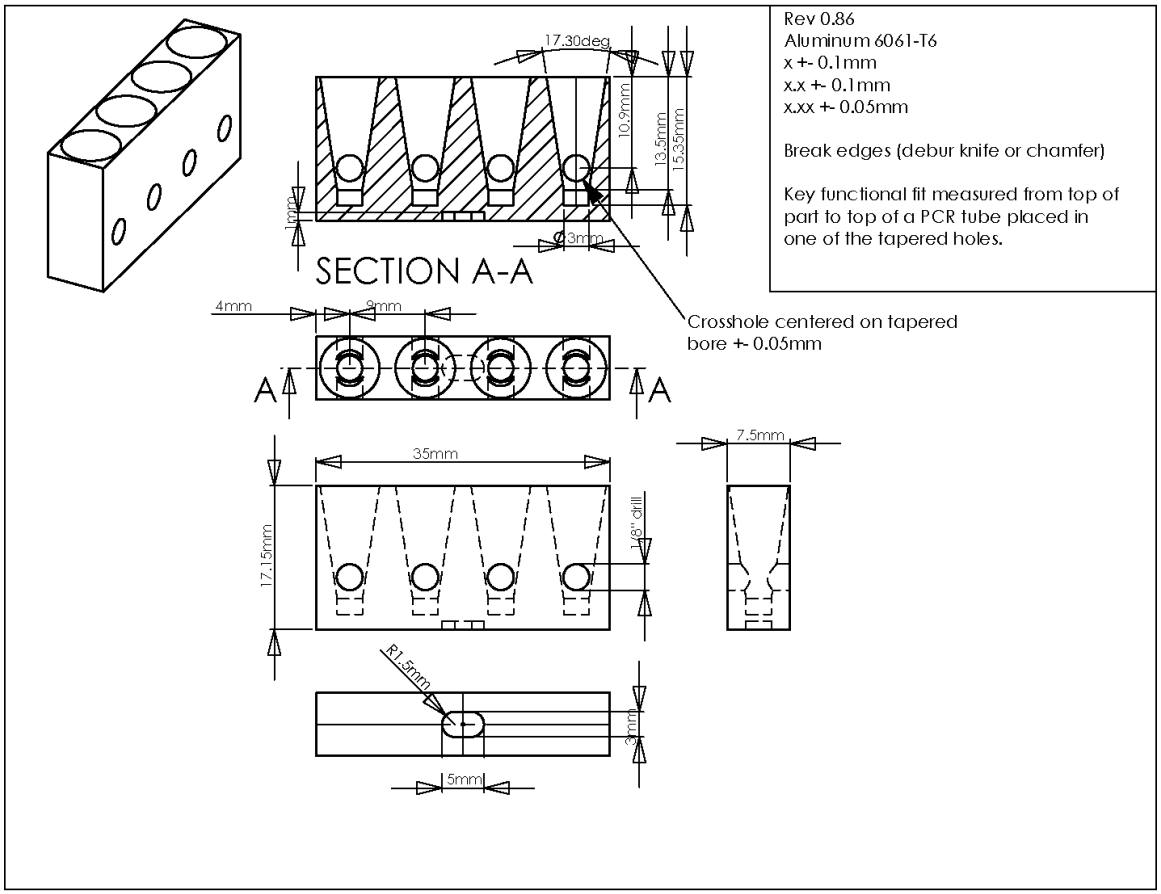

fig. S3 Heat block used in Harmony COVID-19 device. Drawing credit: Bryan Willman.

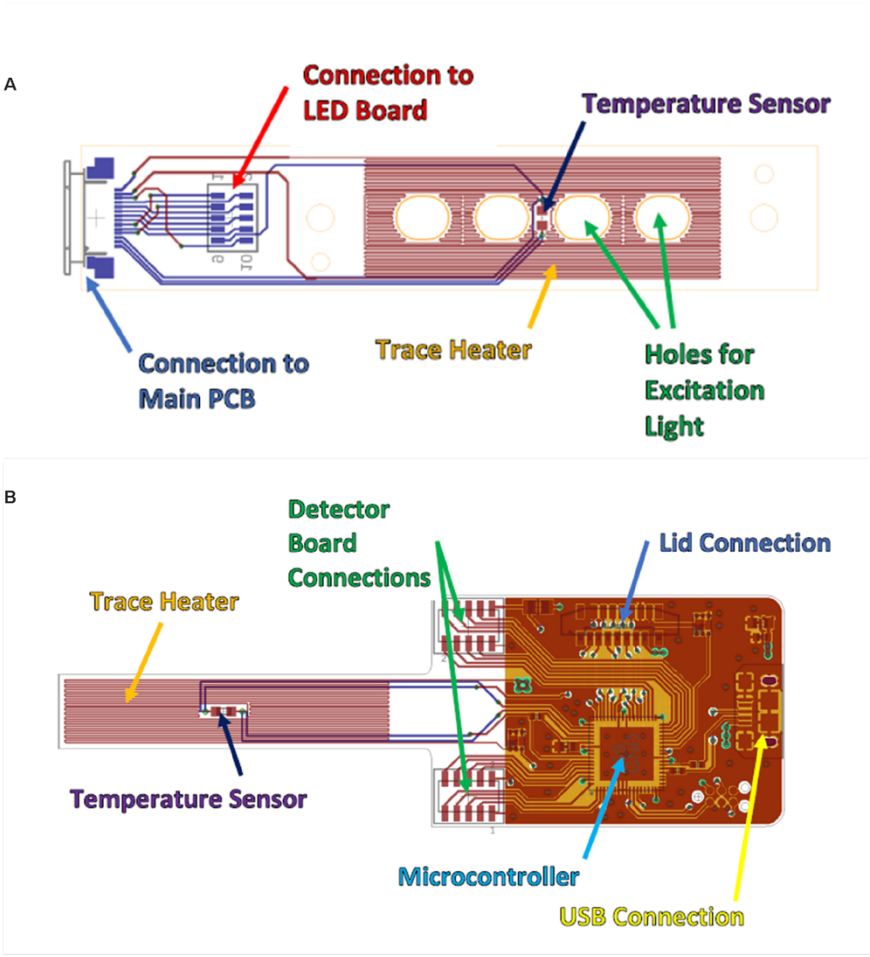

fig. S4 The design of optical and heater circuit boards for the Harmony COVID-19 device. (**A**) LED board (**B**) the detector board

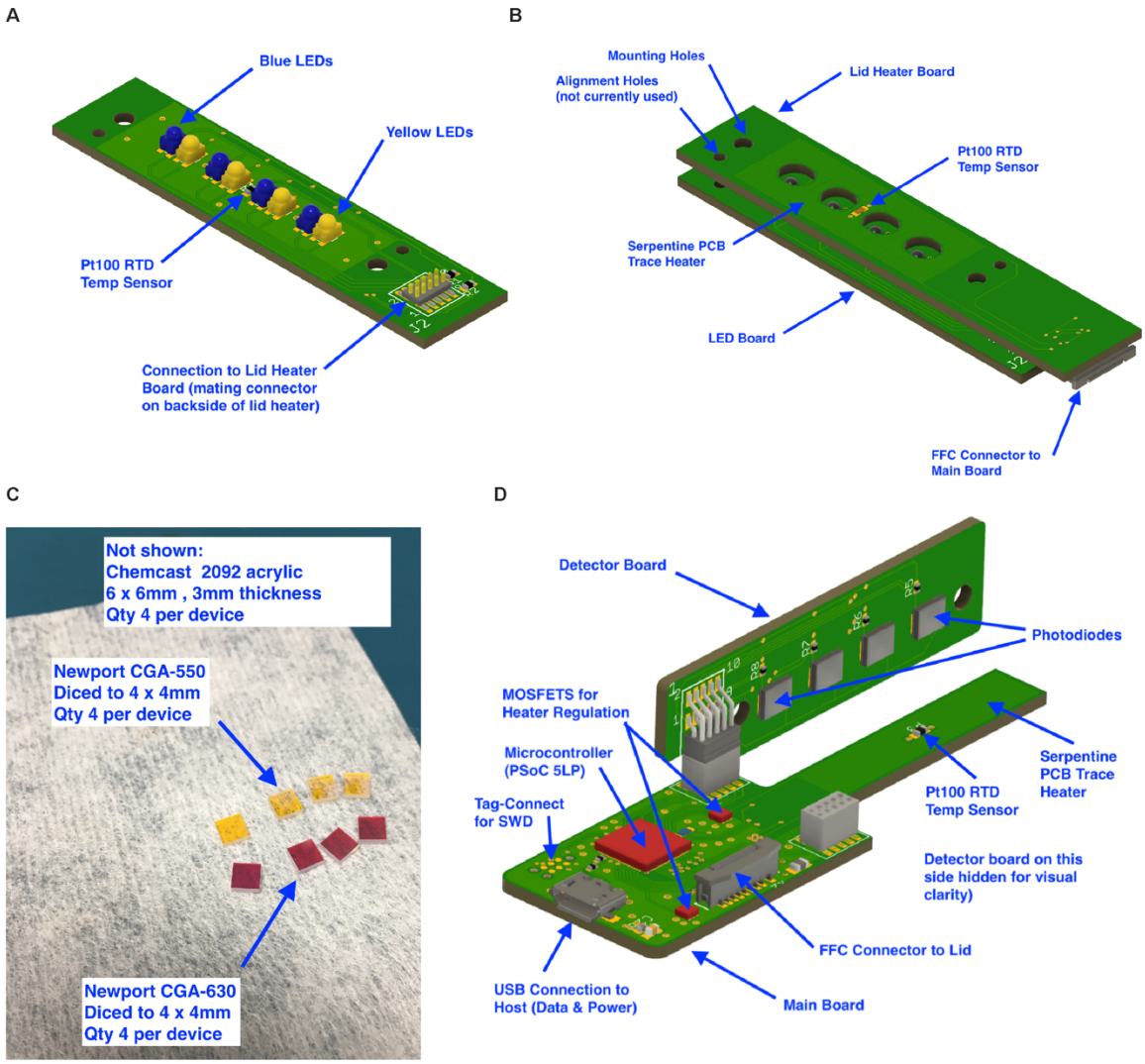

fig. S5 Circuit board assembly and required parts.

(**A**) LED board. (**B**) LED board assembled to the lid heater board. (**C**) Custom-cut filter pieces. (**D**) Detector board and the main board. Each device require the following parts: thick film resistors (RCL12251R20FKEG, RCL12252R20FKEG, CRCW08050000Z0EBC and RCL12254R70FKEG from Vishey; RN73C1J75RBTDF from TE Connectivity; FTS-105-03-F-DV from Samtec; CR0402AJW-472GAS from Bourns), thin film resistors (RN73H1ETTP3003B25 from KOA Speer; ERJ-2RKF22R0X from Panasonic), multilayer ceramic capacitors (C0402C104M4RACAUTO, KEMET;

0603YC105KAT2A, AVX), multilayer ceramic capacitor (GRM188R60J226MEA0D, Murata), USB connectors (10118193-0001LF and 10118192-0001LF, FCI / Amphenol), FFC & FPC connector (52745-1497, Molex), standard yellow LEDs (LY E63B-CBEA-26-1-Z, Osram Opto Semiconductor), standard blue LEDs (150141BS63140, Wurth Elektronik), board-to-board & mezzanine connector (CLP-105-02-F-D and FLE-105-01-G-DV-K-TR, Samtec), FFC/FPC jumper cables (15166-0143, Molex), FFC & FFC connector (52559-1452, Molex), 2 headers & wire Housings (FTSH-105-01-F-DH, Samtec), MOSFET (FDMA410NZ, ON Semiconductor), 2 board-mount temperature sensors (PTS060301B100RP100 from Vishay), ARM Microcontrollers (CY8C5888LTI-LP097, Cypress Semiconductor), Photodiodes (SFH 2201, Opto Semiconductor).

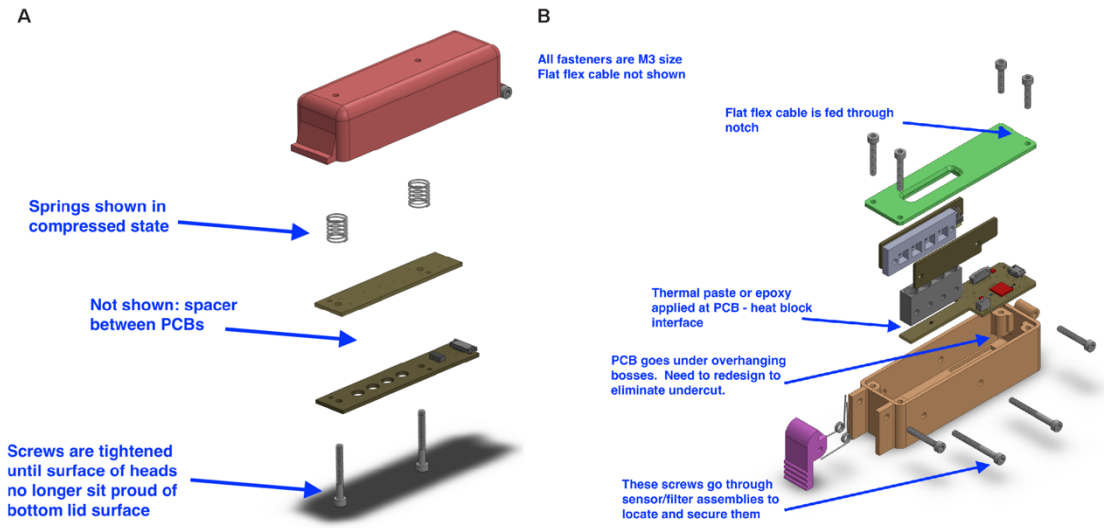

fig. S6 Device assembly.

(**A**) Top part (**B**) Bottom part of the device are assembled using 10 screws, 2 compression springs, and 2 torsion springs (McMaster-Carr, Elmhurst, IL) including: Torsion Spring 90 Degree Angle, Left-Hand Wound, 0.204" OD (9271K109), Torsion Spring 90 Degree Angle, Right-Hand Wound, 0.204" OD (9271K143),Black-Oxide Alloy Steel Socket Head Screw M3 x 0.5 mm Thread, 5 mm Long (91290A110), Black-Oxide Alloy Steel Socket Head Screw M3 x 0.5 mm Thread, 10 mm Long (91290A115), Black-Oxide Alloy Steel Socket Head Screw M3 x 0.5 mm Thread, 15 mm Long (91290A572), Black-Oxide Alloy Steel Socket Head Screw M3 x 0.5 mm Thread, 20 mm Long (91290A123), Black-Oxide Alloy Steel Socket Head Screw M3 x 0.5 mm Thread, 25 mm Long (91290A125), Black-Oxide Alloy Steel Socket Head Screw M3 x 0.5 mm Thread, 30 mm Long, Partially Threaded (91290A130), Music-Wire Steel Compression Springs 0.875" Long, 0.36" OD, 0.296" ID (9434K73).

video S1

Demonstration of transfer pipette workflow incorporated with Harmony COVID-19

video S2

Demonstration of the integrated sampling system workflow with Harmony COVID-19

Both can be played from this slide presentation:

1014 **table S1 Primers, probes, and control sequences.**

1015 For primers and probes F2/B2 sequences are underlined, non-template linker

1016 sequences are italicized, and adapter sequences are in bold.

1017

SARS-Cov-2 NC1 Primers	**Sequence (5' to 3')**
NC1 FIP	CCACTGCGTTCTCCATTC*TTTT*CCCCGCATTACGTTTGGT
NC1 BIP	GCGATCAAAACAACGTCGG*TTAT*TGCCATGTTGAGTGAGAGCG
NC1 LF	TGGTTACTGCCAGTTGAATCT
NC1 LB + T Adapter	**ACCAACACCTCACATCACACATAATA**GGTTTACCCAATAATACTG CGTCTTG
NC1 F3	TGGACCCCAAAATCAGCG
NC1 B3	ATCTGGACTGCTATTGGTGTTA
SARS-CoV-2 NC2 Primer	Sequence
NC2 FIP	CAGCTTCTGGCCCAGTTCCTGTGGTGGTGACGGTAAAATG
NC2 BIP	CTTCCCTATGGTGCTAACAAAG*T*CCAATGTGATCTTTTGGTGTATT CA
NC2 LF	GTAGTAGAAATACCATCTTGGACT
NC2 LB + T Adapter	**ACCAACACCTCACATCACACATAATA**ATATGGGTTGCAACTGAG GGAG
NC2 F3	CTACTACCGAAGAGCTACCAG
NC2 B3	GCAGCATTGTTAGCAGGATTG
SARS-CoV-2 NC3 Primers	Sequence
NC3 FIP	TGTGTAGGTCAACCACGTTC*T*GCTTCAGCGTTCTTCGGA

NC3 BIP	GTGCCATCAAATTGGATGACAAAGGTTTTGTATGCGTCAATATGCTTATTCAG
NC3 LF + T Adapter	**ACCAACACCTCACATCACACATAATA**TCCATGCCAATGCGCGACA
NC3 LB	CCAAATTTCAAAGATCAAGTCAT
NC3 F3	GACCAGGAACTAATCAGACAAG
NC3 B3	GCTTGAGTTTCATCAGCCTTC
IAC (NC1) primer	Sequence
IAC FL + C Adapter	**ACCACACCTACCACCACTAATAACTAA**CTCCAGCCATCCTCACCATC
Target UDP	Sequence
CoV UDP Probe	FITC – CCATCAGCACCAAGACTACCCACCTCGCCACCAA**ACCAACACCTCACATCACACATAATA**
CoV UDP Quencher	TTGGTGGCGAGGTGGGTAGTCTTGGTGCTGATGG– Iowa Black® FQ
Control UDP	Sequence
IAC UDP Probe	Tex615 – CCTGACCACTTCCGAACCCAACCACCTACGACAG**ACCACACCTACCACCACTAATAACTAA**
IAC UDP Quencher	CTGTCGTAGGTGGTTGGGTTCGGAAGTGGTCAGG – BHQ2
IAC Template	Sequence
IAC (NC1) ssDNA	AAT GGA CCC CAA AAT CAG CGA AAT GCA CCC CGC ATT ACG TTT GGT GGA CCC TCT GGA GTC AAT GGG TGG TGC CAG AAT GGA GAA CGC AGT GGG GCG CGA TCA AAA CAA CGT CGG CCC CAA GTT GAT

CTC CAG CCA TCC TCA CCA TCG TTC ACC GCT CTC ACT CAA CAT

GGC AAG AAT TAA CAC CAA TAG CAG TCC AGA TG

1018

1019

1020 **Sample transfer methods at the POC**

1021 Volumetric transfer pipettes are used in POC tests, but we have not identified a unified
1022 dispenser used in commercial pathogen tests. A unified dispenser integrating the swab
1023 and the buffer container in a single unit could reduce opportunities for sample mix-up
1024 when multiple samples are processed simultaneously. A simple workflow is crucial,
1025 especially in busy settings like clinics. However, in our hands, the in-house built
1026 dispenser led to variable dispensed fluid volumes and had a higher failure rate than
1027 those of the transfer pipette method. While the unified dispenser has many attractive
1028 features, we would not recommend using this in-house assembled dispenser unit until
1029 the method has been optimized to achieve a more accurately dispensed volume.

1030

1031 **table S2 Feedback from the HCWs**

1032 Among HCWs, 30% (3/10) reported problems dispensing the fluid using the unified
1033 system. However, 20% (2/10) of HCWs agreed that the unified dispenser offered an
1034 advantage in its similarity to other tools used in healthcare settings, and 30% (3/10)
1035 HCWs were concerned about contaminating the sample or the environment with the
1036 transfer pipette compared to the unified dispenser system. Only 1/10 (10%) HCW
1037 preferred the smallest tube (0.2mL) for either method, and 5/10 (50%) reported that
1038 larger (1.5mL) tubes were helpful for the unified system, while 40% (4/10) of HCWs said

1039 receptacle size did not make a difference when using the transfer pipette, and none
1040 reported preference for tube size when using the unified dispenser system. HCWs
1041 reported higher confidence in correctly completing the second kit compared to the first
1042 kit of each method, indicating a similar learning curve.
1043
1044
1045 (**A**) **User preference for reaction tube size**
1046 Note: Cells with 0% response were left empty to aid data visualization.
1047

Question	**User response, n (%)**				
	0.2 mL	0.5 mL	1.5 mL	0.5mL or 1.5mL	no difference
Which tube size were you most confident using with the unified dispenser swab?		4 (**40%**)	5 (**50%**)	1 (**10%**)	
Which tube size were you most confident using with the transfer pipette?	1 (**10%**)	4 (**40%**)	1 (**10%**)		4 (**40%**)

1048
1049 (**B**) **User responses to survey questions during sample transfer usability testing.**
1050 Users were asked to provide their response on a Likert scale: (1) Not at all, (2) Slightly,
1051 (3) Somewhat, (4) Fairly, (5) Completely. Note: Phrasing of the questions below was
1052 slightly modified to be clear outside of the context of the written protocol/survey (original
1053 survey here). Cells with 0% response were left empty to aid data visualization.

1054

Question	User response, n (%)				
	(1)	**(2)**	**(3)**	**(4)**	**(5)**
How confident were you that you added the **correct amount of liquid** to each reaction tube using the **unified dispenser system?**			3 (**30%**)	3 (**30%**)	4 (**40%**)
How confident were you that you completed the protocol correctly using the **unified dispenser system** with the **first kit**?		2 (**20%**)	1 (**10%**)	4 (**40%**)	3 (**30%**)
How confident were you that you completed the protocol correctly using the unified dispenser system with the second kit?				5(**50%)**	5 (**50%)**
How confident were you that you added the correct amount of liquid to each reaction tube using the **transfer pipette**?			2 (**20%**)	2(**20%**)	6 (**60%**)
How confident were you that you completed the protocol correctly using the **transfer pipette** with the **first kit**?			3 (**30%**)	4 (**40%**)	3 (**30%**)
How confident were you that you completed the protocol correctly				5 (**50%**)	5 (**50%**)

using the **transfer pipette** with the **second kit**?			
How confident were you that you completed the **on-screen instructions correctly**?	1 (**10%**)	4 (**40%**)	5 (**50%**)

(**C**) **User reported errors/challenges between two sample transfer methods.** Cells with no response were left empty to aid data visualization.

	Sample transfer method	
Reported error	Number of occurrences for the **unified dispensing system**	Number of occurrences for the **transfer pipette**
The transfer method was hard to aim at the receiving reaction tube.	1	
Transfer method dripped/leaked before dispensing to the reaction tube.	2	
The materials were too small or difficult to handle.		3
It was hard to execute specific instructions due to unfamiliarity with the sample transfer device.	2	1
Challenging to dispense a consistent amount of fluid.	3	

Not confident liquid was dispensed to the tube.	2
Concerned about contaminating samples or the environment.	3

1059

1060 **table S3 Detailed reagent and device cost at a production scale of 10,000 units**

1061

Item	Supplier	Cost/device (US$)
Detector boards	Macrofab	$7 each x 2 ($14 total)
Main board	Macrofab	$25 each
LED board	Macrofab	$9 each
Lid Heater	Oshpark	$7 each
Heat block	Bryan Willman	$12 each
Housing	Xometry – HP MultiJet Fusion 3D printing, no volume discount	$50 (costs here should be reduced for scale-up production)
Red filters	Newport	$10 each, $40 in total
Green filters	Newport	$20 each, $80 in total
Assembly	N/A	$30 (half an hour assembly time at $60/hour cost)
	Total	**$267 per unit**

1062

1063 **table S4 Consumable costs per test**

Item	Supplier	Costs per kit (US$)

Sampling components ($2 maximum)	Multiple sources	$2
Desiccant	Multiple sources	$0.5
PCR tube	Multiple sources	Negligible
DNA polymerase	Produced in-house	Negligible
Reverse transcriptase	New England Biolabs	$3.5
Thermostable inorganic pyrophosphatase	New England Biolabs	$0.23
Primers	Integrated DNA Technologies	$0.03
Fluorescent probe/quenchers	Integrated DNA Technologies	$0.24
Triton-X100	Sigma-Aldrich	Negligible
dNTPs	New England Biolabs	$0.38
Mannitol	OPS Diagnostics	Negligible
DL-Dithiothreitol (DTT)	Promega	Negligible
Nuclease-free water	VWR	Negligible
1X Tris low-EDTA buffer	VWR	Negligible
Rnasin ribonuclease inhibitor	Promega	$0.71
DNA internal amplification control	Integrated DNA Technologies	$0.01
Cost of goods		**$8.00**

1064

1065